

1. Report No. FHWA/TX-10/0-4624-2		2. Government Accession No.		3. Recipient's Catalog No.	
4. Title and Subtitle EFFECTS OF BENDING AND HEAT ON THE DUCTILITY AND FRACTURE TOUGHNESS OF FLANGE PLATE				5. Report Date March 2007 Published: May 2012	
				6. Performing Organization Code	
7. Author(s) Peter B. Keating and Lee C. Christian				8. Performing Organization Report No. Report 0-4624-2	
9. Performing Organization Name and Address Texas Transportation Institute The Texas A&M University System College Station, Texas 77843-3135				10. Work Unit No. (TRAIS)	
				11. Contract or Grant No. Project 0-4624	
12. Sponsoring Agency Name and Address Texas Department of Transportation Research and Technology Implementation Office P.O. Box 5080 Austin, Texas 78763-5080				13. Type of Report and Period Covered Technical Report: September 2003 – August 2006	
				14. Sponsoring Agency Code	
15. Supplementary Notes Project performed in cooperation with the Texas Department of Transportation and the Federal Highway Administration. Project Title: Performance and Effects of Punched Holes and Cold Bending on Steel Bridge Fabrication URL: http://tti.tamu.edu/document/0-4624-2.pdf					
16. Abstract <p>Bridge fabricators for the Texas Department of Transportation (TxDOT) have occasionally experienced the formation of cracks in flange plate during bending operations, particularly when heat is applied. Bending the flange plate is necessary for certain details used in the fabrication of steel highway girders such as dapped end details. Heat is sometimes used to assist in the bending operation, particularly to help reduce the forces required to bend the plate. This report documents the findings of a TxDOT-sponsored research project that investigated the possible causes of the cracking and developed recommendations to prevent the occurrence of such cracking.</p> <p>The research project investigated the cracking problem using both experimental and analytical studies. The experimental study involved the use of small tensile specimens loaded to different strain levels under varying temperature conditions. Strain levels up to 15 percent were investigated. Temperature conditions included testing at room temperature, 450°F, and 1150°F. The results showed that strain levels above 10 percent generally reduced the ductility and fracture toughness of the plate. Additionally, it was found that the application of heat during the bending process significantly reduced ductility and was the major contributor to the formation of cracks. A finite element study of the heating process was used to extend the results for the experimental study.</p> <p>As a secondary study, the fatigue behavior of non-loaded bolted connection details was investigated along with the influence of plate thickness. These details occur when gusset plates are bolted to flanges of girders. Unlike flange or web splices where the load must transfer out of the main member, the load in these details passes through the main plate, resulting in higher stresses around the bolt holes. Pre-tensioning the bolts normally shields the bolt holes from fatigue damage due to the resulting compressive stress field. This study found that for plate thicknesses greater than 1.0 inches, a reduction in fatigue strength was warranted.</p>					
17. Key Words Steel Plate, Plate Bending, Bridge Fabrication, Heat-Assisted, Bolt Hole Fatigue, Non-Loaded Attachments			18. Distribution Statement No restrictions. This document is available to the public through NTIS: National Technical Information Service Springfield, Virginia 22161 http://www.ntis.gov		
19. Security Classif.(of this report) Unclassified		20. Security Classif.(of this page) Unclassified		21. No. of Pages 94	22. Price

EFFECTS OF BENDING AND HEAT ON THE DUCTILITY AND FRACTURE TOUGHNESS OF FLANGE PLATE

by

Peter B. Keating, Ph.D., P.E.
Associate Research Engineer
Texas Transportation Institute

and

Lee C. Christian
Graduate Research Assistant
Texas Transportation Institute

Report 0-4624-2

Project 0-4624

Project Title: Performance and Effects of Punched Holes and Cold Bending
on Steel Bridge Fabrication

Performed in cooperation with the
Texas Department of Transportation
and the
Federal Highway Administration

March 2007

Published: May 2012

TEXAS TRANSPORTATION INSTITUTE
The Texas A&M University System
College Station, Texas 77843-3135

DISCLAIMER

This research was performed in cooperation with the Texas Department of Transportation (TxDOT) and the Federal Highway Administration (FHWA). The contents of this report reflect the views of the authors, who are responsible for the facts and the accuracy of the data presented herein. The contents do not necessarily reflect the official view or policies of the FHWA or TxDOT. This report does not constitute a standard, specification, or regulation. This report is not intended for construction, bidding, or permit purposes. The researcher in charge of the project was Peter B. Keating, Ph.D., P.E. (TX 103942).

ACKNOWLEDGMENTS

This research was conducted at Texas A&M University (TAMU) and was supported by TxDOT and FHWA through the Texas Transportation Institute (TTI) as part of Project 0-4624, “Performance and Effects of Punched Holes and Cold Bending on Steel Bridge Fabrication.” The authors are grateful to the individuals who were involved with this project and provided valuable assistance, including Heather Gilmer (TxDOT, Research Project Director), Ronnie Medlock (formally TxDOT, Research Project Coordinator), and Jon Holt (TxDOT). The authors are also grateful to Jeff Perry and Matt Potter of the Structures and Materials Testing Laboratory, Zachry Department of Civil Engineering, TAMU, for all their assistance with the experimental portion of this study.

TABLE OF CONTENTS

List of Figures.....	ix
List of Tables	xii
Chapter 1: Introduction	1
1.1 Background	1
1.2 Research Objectives.....	5
Chapter 2: Background.....	7
2.1 General.....	7
2.2 Strain Limitations	7
2.3 Residual Stresses	8
2.4 Thermal Properties of Steel	10
2.5 Heat-Straightening.....	11
2.6 Common Practices by TxDOT Fabricators.....	12
Chapter 3: Laboratory Testing.....	17
3.1 General.....	17
3.2 Test Program.....	18
3.3 Tensile Test Results.....	21
3.3.1 Temperature Condition 1 (TC-1).....	21
3.3.2 Temperature Condition 2 (TC-2).....	21
3.3.3 Temperature Condition 3 (TC-3).....	24
3.3.4 Temperature Condition 4 (TC-4).....	24
3.3.5 Temperature Condition 5 (TC-5).....	27
3.3.6 Fracture Toughness Investigation.....	29
3.4 Conclusions and Recommendations.....	30
Chapter 4: Finite Element Study.....	31
4.1 General.....	31
4.2 Approach to Developing the Finite Element Models.....	31
4.3 Convection Model	32
4.4 Conduction Model.....	33
4.5 Structural Model.....	37
4.6 Thermal Results	38
4.6.1 Through-Thickness Temperature Gradients after Furnace Heating	38
4.6.2 Acetylene Torch Temperature Gradients.....	40
4.6.3 Comparison of Heating Methods	43
4.6.4 Stress-Strain-Temperature Curves	44
4.6.5 Six-Inch Radius Bend	45
4.6.6 Surface Residual Stress Distribution	46
4.6.7 Strain along the Plate's Surface	49
4.6.8 Through-Thickness Stresses	55
4.6.9 Through-Thickness Residual Stresses	59

4.7	Summary and Conclusions	63
4.7.1	Thermal Conclusions	63
4.7.2	Structural Conclusions	63
Chapter 5:	Fatigue Behavior of Non-Loaded Bolted Connections	65
5.1	General	65
5.2	Test Program	65
5.3	Hole Punching	67
5.4	Test Results	70
5.6	Summary	76
5.7	Recommendations	77
Chapter 6:	Conclusions and Recommendations	79
References	81

LIST OF FIGURES

Figure 1-1. Example of Bridge Bent Cap Supporting Both a Steel Girder and Prestressed Concrete Beam (U.S. Highway 59 and Sam Houston Tollway Interchange, Houston, TX).....	2
Figure 1-2. Example of Welded Dapped Girder Detail (Sam Houston Tollway and Interstate 10 Interchange, Houston, TX).....	2
Figure 1-3. Example of Dapped Trapezoidal Box Girder during Fabrication (for U.S. Highway 59, Houston, TX).....	3
Figure 1-4. Standard Dapped Girder Detail Incorporating Bent Flange Plate.....	3
Figure 1-5. View of Cracked Flange Plate As a Result of Bending Operation.....	4
Figure 2-1. Residual Stress Distribution.....	9
Figure 2-2. View of Pyramid-Type Rolling Bending Equipment for Pressure Vessel Plate.....	14
Figure 2-3. View of a Brake Press.....	15
Figure 3-1. Schematic Drawing Showing Difficulty of Obtaining CVN Specimen from Bent Plate.....	18
Figure 3-2. Temperature of TC-3 Being Maintained with a Propane Torch.....	19
Figure 3-3. View of a Gripped Specimen with Attached Clip Gauge.....	20
Figure 3-4. Comparison of Stress-Strain Curves for Temperature Condition 1.....	21
Figure 3-5. Stress-Strain Data for Temperature Condition 2.....	22
Figure 3-6. Specimen Set for Condition 2 (Heated to 1150°F, Tested at Approximately 450°F).....	23
Figure 3-7. Comparison of TC-1 Specimen at 15 Percent Strain and TC-2 Specimen at 11 Percent Strain.....	23
Figure 3-8. Stress-Strain Data for Temperature Condition 3.....	24
Figure 3-9. Stress-Strain Data for Temperature Condition 4.....	25
Figure 3-10. Specimen Set for Condition 4 (Heated to 1150°F, Air-Cooled to Room Temperature and Tested).....	26
Figure 3-11. Comparison between Temperature Condition 1 and Temperature Condition 4 for a Target Strain of 15 Percent.....	26
Figure 3-12. Stress-Strain Data for Temperature Condition 5.....	27
Figure 3-13. Specimen Set for Condition 5 (Cooled to 0°F, Tested while Warming).....	28
Figure 3-14. Comparison of Stress-Strain Curves for Two Specimens That Fractured Prior to Reaching Target Strain (TC-5).....	28
Figure 3-15. CVN Test Data for Temperature Condition 1.....	29
Figure 3-16. Comparison of CVN Test Data between Temperature Condition 1 and Temperature Condition 4.....	30
Figure 4-1. Convection Model.....	33
Figure 4-2. Acetylene Torch Heating.....	34
Figure 4-3. Comparing Heating Temperatures for 2-Inch Plate.....	35
Figure 4-4. Comparing Through-Thickness Stresses.....	36
Figure 4-5. Conduction Model.....	37
Figure 4-6. Structural Model.....	38
Figure 4-7. Through-Thickness Temperature Distribution for 1-Inch Plate.....	39
Figure 4-8. Through-Thickness Temperature Distribution for 1.5-Inch Plate.....	40
Figure 4-9. Through-Thickness Temperature Distribution for 2-Inch Plate.....	40

Figure 4-10. 1200°F Surface Temperature 2-Inch Plate.....	41
Figure 4-11. Acetylene Torch Through-Thickness Temperature Distribution for 1-Inch Plate.....	42
Figure 4-12. Acetylene Torch Through-Thickness Temperature Distribution for 1.5-Inch Plate.....	43
Figure 4-13. Grade 50 Stress-Strain-Temperature Curves.....	44
Figure 4-14. Grade 70 Stress-Strain-Temperature Curves.....	45
Figure 4-15. Load Steps.....	46
Figure 4-16. Surface Residual Stress 1-Inch Plate - 50 ksi.....	47
Figure 4-17. Surface Residual Stress 1.5-Inch Plate - 50 ksi.....	48
Figure 4-18. Surface Residual Stress 2-Inch Plate - 50 ksi.....	48
Figure 4-19. Surface Strain 1-Inch Plate - 50 ksi.....	50
Figure 4-20. Surface Strain 1.5-Inch Plate - 50 ksi.....	51
Figure 4-21. Surface Strain 2-Inch Plate - 50 ksi.....	51
Figure 4-22. Surface Strain at a Point 1-Inch Plate - 50 ksi.....	53
Figure 4-23. Surface Strain at a Point 1.5-Inch Plate - 50 ksi.....	53
Figure 4-24. Surface Strain at a Point 2-Inch Plate - 50 ksi.....	54
Figure 4-25. Through-Thickness Stress Cold Bend - 50 ksi.....	56
Figure 4-26. Through-Thickness Stress 10 Minute Cooling - 50 ksi.....	57
Figure 4-27. Through-Thickness Stress 1100°F Uniform Temperature - 50 ksi.....	57
Figure 4-28. Through-Thickness Stress 1200°F Surface Temperature - 50 ksi.....	58
Figure 4-29. Through-Thickness Residual Stress Cold Bend - 50 ksi.....	60
Figure 4-30. Through-Thickness Residual Stress 10 Minute Cooling - 50 ksi.....	61
Figure 4-31. Through-Thickness Residual Stress 1100°F Uniform - 50 ksi.....	62
Figure 4-32. Through-Thickness Residual Stress 1200°F Surface Temperature - 50 ksi.....	62
Figure 5-1. Specimen with Bolted Gusset Plate.....	66
Figure 5-2. 1.5 Million Pound Capacity Load Frame with Non-Loaded Bolted Connection Specimen.....	67
Figure 5-3. View of Hole Punching Operation with Specimen C-1.....	68
Figure 5-4. Close-Up View of Punch and Die for Specimen Hole Punching.....	68
Figure 5-5. Plot of Punch Load versus Displacement for Plate Thicknesses of 0.5, 0.75, and 1.0 Inches.....	69
Figure 5-6. Hole Slugs for Three Plate Thicknesses Resulting from Punching Operation.....	69
Figure 5-7. Typical Crack Orientation for Specimens with Bolted Gusset Plate (Specimen D-1).....	72
Figure 5-8. Typical Crack Orientation for Thin Plates (<1.0 Inches) with a Gusset Plate (Specimen B-4).....	72
Figure 5-9. Typical Crack Orientation for Thick Plates (≥1.0 Inches) with a Gusset Plate (Specimen E-3).....	73
Figure 5-10. Stress Range vs. Number of Cycles to Failure for 0.5-Inch Thick Specimens.....	73
Figure 5-11. Stress Range vs. Number of Cycles to Failure for 0.75-Inch Thick Specimens.....	74
Figure 5-12. Stress Range vs. Number of Cycles to Failure for 1.0-Inch Thick Specimens.....	74
Figure 5-13. Stress Range vs. Number of Cycles to Failure for 1.25-Inch Thick Specimens.....	75

Figure 5-14. Stress Range vs. Number of Cycles to Failure for 1.5-Inch Thick Specimens..... 75
Figure 5-15. Stress Range vs. Number of Cycles to Failure for 2.0-Inch Thick Specimens..... 76

LIST OF TABLES

Table 2-1. Resulting Extreme Fiber Strains.....	8
Table 2-2. Common Bend Angles as a Function of Plate Thickness.....	13
Table 4-1. Comparison of Surface Strains.....	49
Table 4-2. Five Percent Strain.	55
Table 5-1. Test Matrix and Results for Fatigue Behavior of Non-Loaded Bolted Connections. .	71
Table 6-1. Recommended Minimum Bend Radii by Plate Thickness.....	79

CHAPTER 1: INTRODUCTION

1.1 BACKGROUND

The highway bridge industry commonly uses steel plates to fabricate built-up girders that can span around horizontal curves and over longer distances than can be accomplished with prestressed concrete beams. Large, multi-level highway interchanges often employ both steel and prestressed concrete spans. Steel girders are usually deeper in cross section than prestressed concrete beams because of their greater span lengths. The point of transition between the two types of spans requires the end of the steel girder to be reduced in cross section depth so that both the prestressed concrete beam and steel girder can seat on a common bent cap. [Figure 1-1](#) shows an example of a bent cap with both types of members. A steel girder with an end transition is commonly referred to as a dapped girder.

The reduction in girder depth is possible since the moment capacity requirements are less at the end of the span than at other locations. Shear capacity requirements, though higher at the end of the girder, can still be met in the dapped region by stiffening or increasing the thickness of the web plate.

The use of dapped girders by the Texas Department of Transportation (TxDOT) has increased significantly over the past 10 years as highway construction projects in urban areas have required more complex interchange designs. TxDOT has used several end transition details for their dapped girders. [Figure 1-2](#) shows a detail that requires extensive welding and stiffening. Consequently, its use has fallen out of favor. A more common detail is one in which the bottom flange is bent to form the transition, as shown in [Figure 1-1](#), for example. Mechanically bending the flange plate about its weak axis is preferred, due to economic and performance reasons, over welding the plates together with a complete penetration groove weld to form a kink. The groove weld requires plate preparation prior to welding and nondestructive testing upon its completion. Additionally, the completed welded flange splice may still require bending to correct the transition angle for weld shrinkage and distortion.

The slope of the transition can range from 1:5 to vertical. The vertical, or 90-degree bend, has been gaining popularity for aesthetic reasons. The bottom flange more closely follows the lower vertical face of the bent cap and minimizes the appearance of the transition. (This detail

also simulates the appearance of a similar detail used for TxDOT's prestressed concrete U-beams.) An example of the 90-degree bend used at the end of a trapezoidal box or tub girder is given in [Figure 1-3](#). Based on structural considerations, it has been recommended that a slope no greater than 1:1 be used ([Fry et al. 2005](#)). One of two current standard TxDOT dapped girder details allows for a radius of 15 times the plate thickness as the top bend and the use of a welded plate intersection at the bottom (see [Figure 1-4](#))



Figure 1-1. Example of Bridge Bent Cap Supporting Both a Steel Girder and Prestressed Concrete Beam (U.S. Highway 59 and Sam Houston Tollway Interchange, Houston, TX).



Figure 1-2. Example of Welded Dapped Girder Detail (Sam Houston Tollway and Interstate 10 Interchange, Houston, TX).

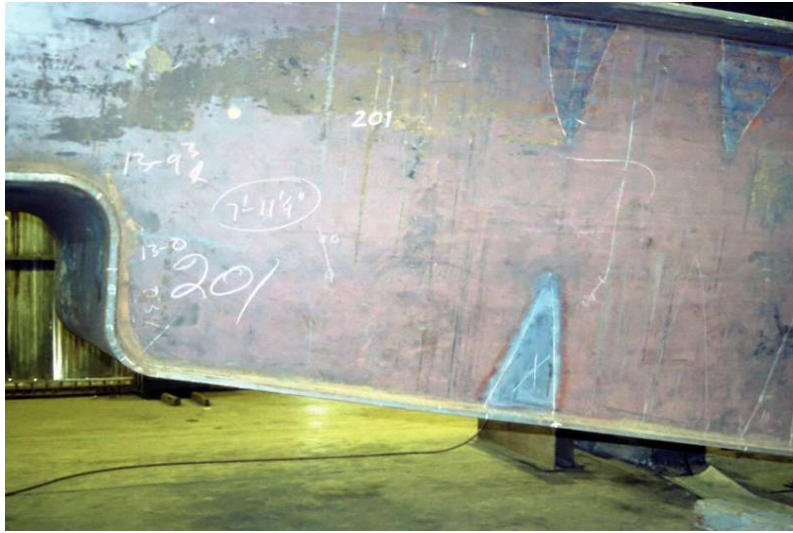
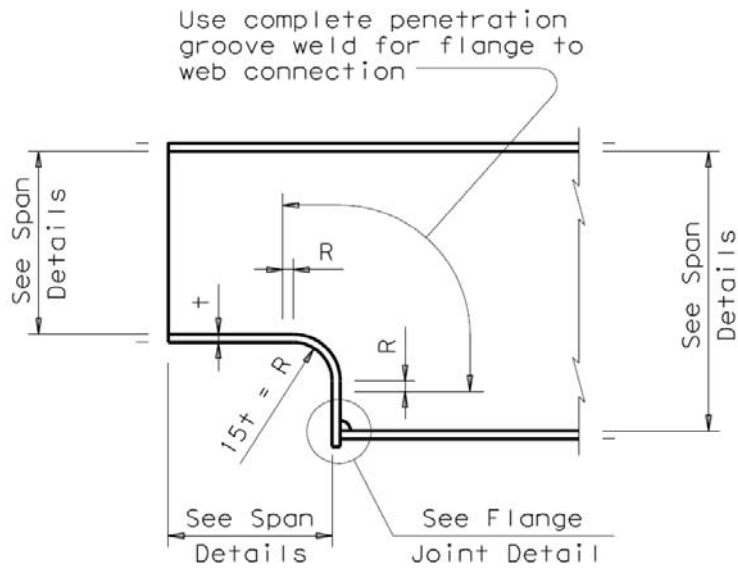


Figure 1-3. Example of Dapped Trapezoidal Box Girder during Fabrication (for U.S. Highway 59, Houston, TX).



TYPE 2

DAPPED GIRDER END DETAILS

(Plate Girders Only)

Figure 1-4. Standard Dapped Girder Detail Incorporating Bent Flange Plate.

Depending on several parameters, such as flange thickness and width, bending angle and radius, and plate yield strength, the bending operation may involve several load-bending cycles as well as the application of heat. The actual process used to bend the plate is a function of fabricator equipment and preference. Heat is often used to reduce the bending strength of the steel when the required bend forces exceed the capacities of the fabricator equipment. This is common for trapezoidal box girders where the bottom flange width can exceed five or more feet.

Bending the flange causes the formation of residual stresses and increases the possibility of cracking due to the high strains experienced at the extreme fibers. [Figure 1-4](#) provides an example of a cracked flange resulting from the bending process. Because of the cracking problem, American Association of State Highway and Transportation Officials (AASHTO) specifications do not allow cold-bending for fracture-critical materials ([AASHTO/NSBA 2002](#)). This makes it necessary for dapped girder flanges to be bent at elevated temperatures, for they are commonly designated as fracture critical. Cracking even at elevated temperatures is still a major concern; factors that play a role in the plate's susceptibility to cracking is how fast the plate is loaded and the temperature distribution through the plate's thickness during the bending process. As the loading rate increases, so does the likelihood of cracking and local distortions occurring in the bent plate ([AASHTO/NSBA 2002](#)).



Figure 1-5. View of Cracked Flange Plate As a Result of Bending Operation.

1.2 RESEARCH OBJECTIVES

The primary objective of the current study is to gain a better understanding of the plate bending operation through experimental and analytical efforts. The knowledge gained from these efforts will be used to develop guidelines for plate bending operations that will reduce or eliminate the possibility of crack formation. This will result in more economical bridge girder fabrication.

As part of the overall efforts of Project 0-4624, the present study also investigates the fatigue behavior of non-loaded bolted connections. These connections differ in how they transfer load. Consequently, the bolt holes are subject to higher levels of stress concentration than connections designed for load transfer via the faying surfaces. This study will determine if there is a plate thickness effect (increasing plate thickness) that may reduce the fatigue strength of non-loaded bolted connections to that below AASHTO Fatigue Category B.

CHAPTER 2: BACKGROUND

2.1 GENERAL

Fabricating steel plates by bending them into various forms is common throughout the steel manufacturing industry. Because of this various standards have been developed over the years for guidance during the manufacturing process. It is important to have an understanding of current industry standards and past research related to plate bending in order to have a starting point from which to determine what might be the cause of cracking of the bent flange plate of dapped girders.

2.2 STRAIN LIMITATIONS

As steel is bent to different degrees of severity it becomes necessary at some point to heat-treat the steel to recover some of its lost material properties. For carbon and low-alloy steel vessels, section UCS 79 of the American Society of Mechanical Engineers ([ASME 2004](#)) Boiler and Pressure Vessel Code specifies 5 percent of extreme fiber elongation from the as-rolled condition be used to determine whether it is necessary to heat-treat steel upon completion of the bending process. The equation used in the ASME Boiler and Pressure Vessel Code to determine the plate's extreme fiber elongation for a single curvature is given by:

$$\% \text{ extreme fiber elongation} = \frac{50t}{R_f} \left(1 - \frac{R_f}{R_o} \right) \quad (2-1)$$

Where:

t = plate thickness (inches),

R_f = final bend radius (inches), and

R_o = initial bend radius (inches).

R_o is equal to infinity for flat plates. This 5 percent strain limit dates back to early steel manufacturing when steel had property degrading imperfections in higher concentrations than what is found in today's manufactured steel. Because of the improvement in the manufacturing

process of steel, some studies suggest that the 5 percent strain limit is too conservative and should be increased to as high as 7 percent (Bala and Malik 1983, Blondeau et al. 1984). The boiler and pressure vessel industry has not accepted this 7 percent strain level, in part because of the catastrophic consequences of failure.

Using Eq. (2-1) to determine extreme fiber strain shows that bending a plate to a 6-inch radius causes the extreme fibers to exceed the 5 percent strain limit proposed by the Boiler and Pressure Vessel Code, shown in Table 2-1. Equation (2-1) further indicates that the 7 percent limit proposed for use on steel having a cleaner metallurgical composition is also exceeded. To limit the strain to 5 percent, a plate no thicker than 0.60 inches can be bent. If a 7 percent limit is used, the plate thickness cannot exceed 0.84 inches.

Table 2-1. Resulting Extreme Fiber Strains.

Plate thickness (in.)	ASME Code
1.0	8.3%
1.5	12.5%
2.0	16.7%

2.3 RESIDUAL STRESSES

Residual stresses can occur when a material is loaded beyond the yield point into the inelastic region of the stress-strain curve. Upon unloading, those stresses that remain are the residual stresses. If a material deforms into the inelastic region it will undergo permanent deformation; the residual stresses (σ') are determined by taking the difference between the initial stress (σ) and the change in stress ($\Delta\sigma$) after unloading (Kervick and Springborn 1966).

$$\sigma' = \sigma - \Delta\sigma \tag{2-2}$$

One detrimental effect that residual stresses can have on a plate's mechanical properties is that these stresses may be a source of cracking and stress corrosion. Residual stresses also reduce the apparent stiffness of the material, as yielding occurs at lower stress levels upon reloading. Cracking and stress corrosion occur where the tensile residual stresses on the inside surface of the plate bend are located (Weng and White 1990a). The zigzag distribution of

residual stresses through the plate's thickness after the plate is unloaded, shown in [Figure 2-1](#), is common for any structural member, with the magnitude of the residual stresses dependent on the bending loads.

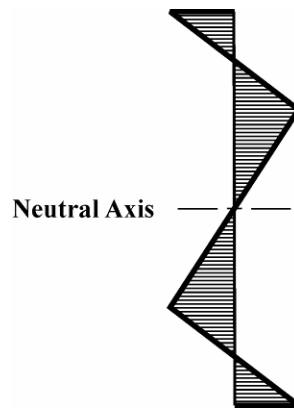


Figure 2-1. Residual Stress Distribution.

When small bending radii are obtained from the bending process of high-strength structural steel, it has been observed that the compression side of the plate is thicker than that of the tension side, causing the neutral axis to move from the centroid of the plate to as much as 5 percent of the plate's thickness ([Weng and White 1990b](#)). The movement of the neutral axis causes an increase in the magnitude of stresses on the tension side of the plate. This increase is brought about because the sum of the stresses through the plate's thickness must equal zero to produce stress equilibrium of the plate when the plate is free of external loads.

Another factor that plays a role in the amount of residual stresses that occur after unloading of the plate is springback. Springback is the difference between the angle at which the plate is bent at maximum load and the angle of the plate observed after unloading. Springback in practice makes it necessary to load a plate past the desired shape during the loading stage so that after unloading the plate will be bent to the correct position. A key part of calculating how much further a plate should be bent depends on the yield strength of the material. As the material's yield strength increases so does the material's springback after unloading. Another factor in determining the amount of springback the plate experiences is that as the bend radius becomes more severe the amount of springback occurring after the plate is unloaded decreases ([Weng and White 1990b](#)). This reduction in springback is caused by the decrease in the elastic portion of the

bent plate. An equation for predicting the amount of springback after cold-bending is also referred to by [Weng and White \(1990b\)](#) as:

$$\frac{R}{r} = 4 \left(R \sigma_y \frac{1-\mu^2}{Et} \right)^3 - 3 \left(R \sigma_y \frac{1-\mu^2}{Et} \right) + 1 \quad (2-3)$$

Where:

R = bend radius to the plate's neutral surface before springback (inches),

r = bend radius to the plate's neutral surface after springback (inches),

σ_y = yield stress (ksi),

E = Young's modulus (ksi),

t = thickness (inches), and

μ = Poisson's ratio.

With proper heat-treatment after the loading and unloading processes are completed, the residual stresses can be reduced and the steel's original material properties can be restored.

2.4 THERMAL PROPERTIES OF STEEL

The mechanical properties of structural steel change with a change in temperature. This change in mechanical properties may lead to changes in the stresses and strain distributions in both the loading and unloading cycles of the bending process. The major areas of concern when temperature is involved are the changes in the steel's stress-strain behavior, phase changes, and thermal coefficient of expansion.

The stress-strain curve of steel plays an important role in determining the stresses and deformation that will occur for a given load. The stress-strain curves for steel change along with changes in temperature. Therefore, it is important to determine as accurately as possible the stress-strain curve for a particular steel grade. Experimental data are the best and most accurate way of determining stress-strain curves for various temperatures, but, unfortunately, it is not always possible to obtain those data. For this reason, several stress-strain-temperature relationships have been proposed. The most commonly used relationships today in industry are those proposed by Lie and the Eurocode. The Lie relationship, most widely used in North America, uses a bilinear curve to model the entire stress-strain curve ([Lie 1992](#)), while the

Eurocode 3, most widely used in Europe, models the stress-strain curve with seven linear and parabolic equations (Poh 2001). Other studies, such as the one conducted by Poh, depict the entire stress-strain-temperature behavior with a single equation (Poh 2001).

As steel increases in temperature it expands in all directions if the material is left unconstrained. If the expansion is confined, large compression stresses will develop. The coefficient of thermal expansion is generally accepted to be $7.8 \times 10^{-6}/^{\circ}\text{F}$ for fire analysis of structures (Cooke 1988), and this value is assumed to be constant as the temperature increases from room temperature to 1200°F.

2.5 HEAT-STRAIGHTENING

Heat-straightening is the use of heat to manipulate damaged steel into the desired shape without adversely affecting the material properties of the steel. Heat-straightening is commonly used in the bridge industry today to repair damaged bridge beams in the field as well as to correct welding distortion during fabrication. Important aspects of heat-straightening that have to be addressed are the pattern and temperature to which to heat the beam, the method of applying the heat to the member, and determining whether restraining forces should be used.

Typical heating patterns for repairing damaged beams are (Avent 1992):

- vee heating – used for straightening strong axis bends (see Figure 1-3, for example),
- edge heating – used for making smooth and gentle plate bends,
- line heating – used for repairing a weak axis plate bend, and
- spot heating – used for repairing localized bulges and dents in a plate.

According to Avent (1989), when using these heating patterns in repairing damaged steel it is important to apply the heat as evenly as possible and only to the region where plastic deformation has occurred so that when the beam is cooling the proper residual stresses will develop to obtain the desired outcome. For bending plate during fabrication, heating should be localized to those regions expected to undergo plastic deformation.

The temperature that the plate reaches during the process of heat-straightening should never exceed 1300°F, for if the steel exceeds this temperature it is in danger of undergoing a phase change in the molecular structure of the steel from a body-centered cubic to a face-

centered cubic. This phase where the molecular structure becomes face-centered is commonly called the martensite phase, and it increases the steel's susceptibility to brittle fracture during repeated loadings (FHWA 1998). For this reason the AASHTO/NSBA steel bridge fabrication guide specification limits the temperature that the steel can reach during the heating process to 1200°F to avoid this phase change (AASHTO/NSBA 2002).

During heat-straightening, a major concern is that the temperature is achieved as rapidly as possible without buckling or overheating the material to allow the proper contraction forces to occur when the plate is cooled (TXDOT 2004). The recommended application method for applying heat during heat-straightening changes as the thickness of the material that is being straightened changes. For member thicknesses of less than 1 inch it is recommended that a single orifice be used to apply heat, but when the thickness of the steel exceeds 1 inch it is recommended that a rosebud be used for apply heat to a member (FHWA 1998).

2.6 COMMON PRACTICES BY TXDOT FABRICATORS

As part of the current study, bridge fabricators (ASIC Category III) that commonly fabricate bridge girders for TxDOT were surveyed to determine their methods and experiences with plate bending. In general, the limits on the maximum plate thickness that could be bent by these fabricators were dependent on the capacities of their equipment and the success that they have had bending plate. A more detailed summary of their replies is provided below.

Fabricator #1

- Does not cold-bend any significant material.
- Heat-bends up to 1.25 inches (no temperature given).
- Subcontracts cold-bending of A709 Grade 50 (non-FCM) up to 2.5 inches × 20 inches.

Fabricator #2

- Maximum thickness for cold-bending is 2.5 inches.
- Has experienced cracking or tearing in 8 of 32 pieces, 1.5 inch thick, with heat assistance at a temperature of 700°F. The plates were used in the dapped bottom flange of tub girders with a 90-degree bend and a tight radius.

- Subcontractor for Fabricator #2 uses a heat-assisted temperature of 400°F and has not experienced cracking issues.

Fabricator #3

- Practical limit of 1 inch for cold-bending.
- Will heat-assist (1000°F) for bending thicknesses greater than 1 inch.
- Recognize radius of curvature to be a function of plate thickness and degree of bending.
- Inspection of plate edges prior to bending.
- Sharp edges on plate edges are ground out to prevent cracking (as required by TxDOT specifications).
- Common bend angles as a function of plate thickness are given as shown in [Table 2-2](#).

Table 2-2. Common Bend Angles As a Function of Plate Thickness.

Bend Angle (degrees)	Radius of Bending
61 – 90	1.0 × plate thickness
91 – 120	1.5 × plate thickness
120 – 150	2.0 × plate thickness

Fabricator #4

- Factors that control the ability to cold-bend include: tonnage, width of press break, width of plate, and radius of bend.
- Limits on cold-bending are partially controlled by equipment limitations.
- Maximum cold-bending thickness is 0.75 inch (72 inches wide) A709 Grade 50 for a 90-degree bend (using a step-break method).
- Maximum heat-assisted (900° to 1000°F) thickness is 1.25 inches (85 inches wide) A709 Grade 50 (using a step-break method).

- Subcontracts with a vendor that has cold-bent non-FCM A709 Grade 50 up to 2.75 inches × 20 inches.

The review of fabricator practices indicated that cold-bending was preferred, but the use of heat during the bending process became necessary when plate thickness and or width resulted in bending forces that exceeded the capacity of the equipment (heat-assisted cold bending). When cracking occurred, it did so when heat was used during the bending process.

As part of the study, a tour of a facility that bends plate as part of its process for the fabrication of pressure vessels was taken. At this facility two methods of bending plate were employed: pyramid-type roll bending and brake press. [Figure 2-2](#) shows the pyramid-type roll bend equipment, while [Figure 2-3](#) is a view of a brake press. The pyramid-type rolling bend provides a more continuous curvature of the plate than the brake press, resulting in a lower level of bending stresses and strains. However, this equipment is generally not used by bridge fabricators and would only be used if the plate bending work was subcontracted to a company with the equipment. It was of interest that a representative of the visited facility mentioned that the only time they had occurrences of plate cracking during bending was when heat was used. Cold-bending did not result in cracked plates.



Figure 2-2 View of Pyramid-Type Rolling Bending Equipment for Pressure Vessel Plate.



Figure 2-3 View of a Brake Press.

CHAPTER 3: LABORATORY TESTING

3.1 GENERAL

A test program was developed to study the plate bending phenomenon in a controlled laboratory setting. The objective of the experimental program was to use typical constructional bridge steel to study the effects of different temperature conditions on the following:

- stress-strain behavior in the inelastic region,
- ductility and susceptibility to form crack at high strain levels, and
- fracture toughness through the use of Charpy V-Notch (CVN) specimens.

Initially, full-scale plate specimens were to be used in the study. However, after a series of preliminary tests, it quickly became apparent that the use of full-scale plate specimens would not allow accurate measurements of the flexural strains or provide a means of obtaining sustainable specimens for evaluating changes to the fracture toughness of the steel (CVN specimens). Given that the outer bending fiber strains far exceeded the yield strain, coupled with the curvature of the plate, there was no practical or accurate means of measuring the level of strains as a result of the bending process. Additionally, machining CVN specimens from bent plate has limitations. First, a correctly sized specimen cannot be obtained from the outside curvature of a bent plate, as illustrated schematically in [Figure 3-1](#) (although it can be obtained from the inside curvature). The notch of the CVN specimen must be oriented perpendicular to the direction of the bending strains. Other types of fracture toughness specimens exist, such as compact tension specimens. However, in addition to significantly higher costs, their use did not solve the second limitation of this type of test: the notch depth is below the region that experiences the greatest strain and is therefore of most interest.

The bending of plate results in the localized triaxial state of stress. The formation of cracks would coincide with the steel reaching its tensile strength. Therefore, for the purposes of this study, it is assumed that the onset of necking is an indication that the steel has become susceptible to crack formation.

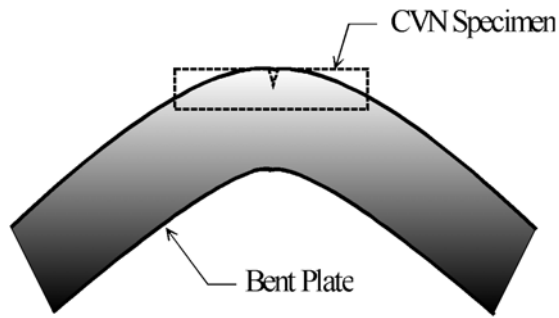


Figure 3-1. Schematic Drawing Showing Difficulty of Obtaining CVN Specimen from Bent Plate.

3.2 TEST PROGRAM

To obtain more applicable fracture toughness results, as well as to allow for accurate measurements of strain, researchers developed an alternative testing method. This method involved the use of small specimens of square cross section ($3/8$ inch \times $3/8$ inch \times 8 inches) cut from unbent steel plate. These specimens were then loaded in axial tension to different strain levels and under different temperature conditions. Five different levels of strain were investigated: 9, 11, 13, and 15 percent (in./in.). These strain levels are often referred to as target strains in the current study, as these levels could not always be achieved prior to necking or fracture at certain temperature conditions. For the steels investigated in this study (primarily American Society of Testing and Materials [ASTM] A572 Grade 50 or equivalent), the maximum strain level that could be achieved without visible signs of necking under the most favorable temperature condition was 15 percent. Therefore, higher strain levels could not be achieved. Five different temperature conditions were investigated:

1. room temperature,
2. heated to 1150°F, cooled to 400°-500°F at testing,
3. heated to 1150°F, tested at 1150°F,
4. heated to 1150°F, cooled to room temperature and tested, and
5. cooled to 0°F, tested while warming.

These temperature conditions were selected to represent different situations that could occur during the fabrication of a highway girder and the plate bending process. For example,

Temperature Condition 2 (TC-2) simulated where the plate to be bent is heated in a furnace but allowed to cool during bending. TC-5 simulated where the plate is stored outside by a fabricator located in a colder climate and brought inside for bending without any heat assistance.

The room temperature for TC-1 was approximately 75°F. Heating the specimens to 1150°F (TC-2, TC-3, and TC-4) was performed by heating them in a small temperature-controlled furnace for a minimum of 6 hours. Specimens tested at a temperature range of 400°-500°F (TC-2) were allowed to air-cool to this range while gripped in the test machine. The specimen's temperature was continuously monitored using a non-contact laser temperature instrument. Once the upper limit of the temperature test range was reached, loading of the specimen commenced. Temperatures of specimens tested at 1150°F (TC-3) were maintained by using a propane torch and monitoring the temperature (Figure 3-2).

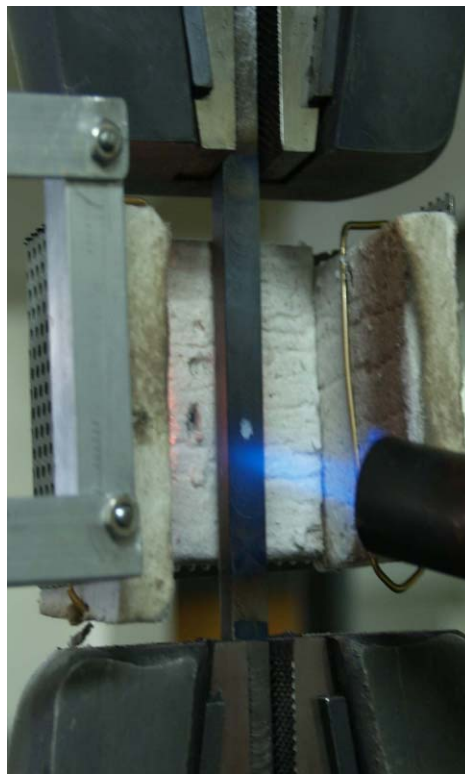


Figure 3-2. Temperature of TC-3 Being Maintained with a Propane Torch.

For specimens not tested at elevated temperatures (TC-1 and TC-5), a clip gauge was used to measure the strain directly (see Figure 3-3). The gauge length of the clip gauge was 1.0 inch. For specimens tested at elevated temperatures, the strain was approximated using the

measured displacement of the test frame fixtures. Additionally, these displacements were correlated to the clip gauge measurements obtained from the specimens tested at room temperature, given that the testing was performed under displacement-controlled (inches per minute) testing conditions. The gage lengths of the specimens were 3.0 inches.



Figure 3-3. View of a Gripped Specimen with Attached Clip Gauge.

For each specimen tested, the applied load, test frame displacement, and, when possible, clip-gauge strains were continuously recorded. The specimens were loaded until the target strain was reached, or until the specimen started to neck or it fractured. A machine displacement rate of 1.0 in./min was used for all specimens.

3.3 TENSILE TEST RESULTS

3.3.1 Temperature Condition 1 (TC-1)

The set of tensile tests for TC-1 (tested at room temperature) was used to establish a baseline for material behavior. In general, the test results showed that the steel provided good ductility even at the higher levels of strain (11 to 15 percent). No indication of necking in the specimens was evident by visual inspection. Representative stress-strain data are provided in [Figure 3-4](#) for each of the target strains (7, 9, 11, 13, and 15 percent). Examination of [Figure 3-4](#) indicates that necking begins at approximately 15 percent. Note that common high-strength, low-alloy steels do not display a distinct plateau of the stress-strain curves at the onset of yielding.

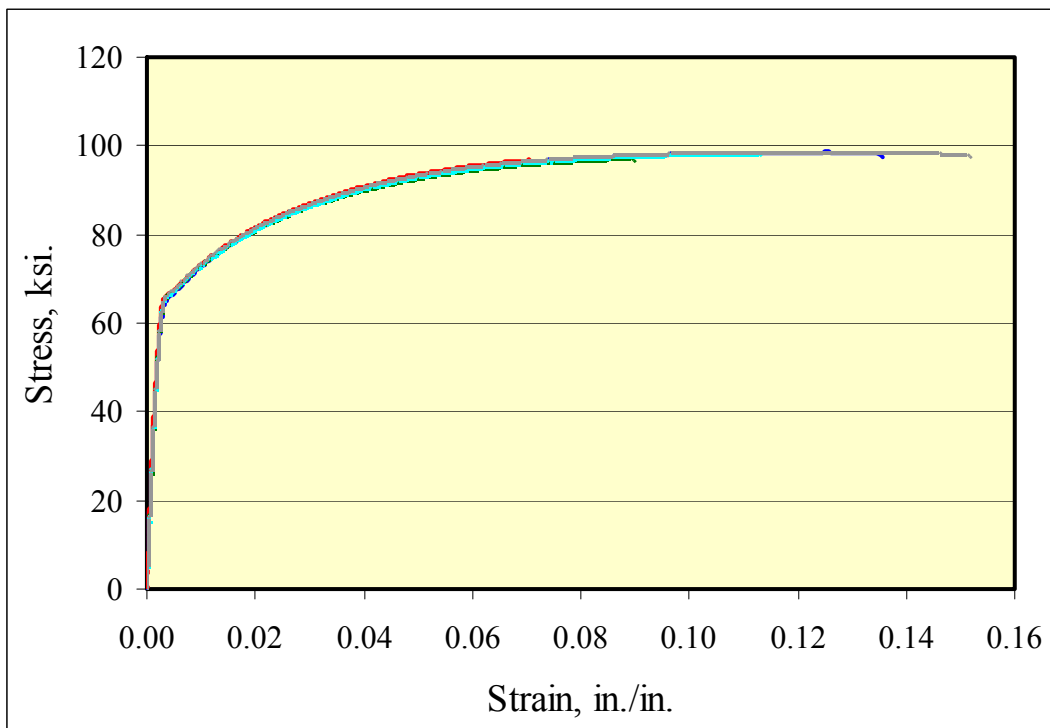


Figure 3-4. Comparison of Stress-Strain Curves for Temperature Condition 1.

3.3.2 Temperature Condition 2 (TC-2)

The results from the stress-strain data for TC-2 (specimens heated to 1150°F, tested at 400°-500°F) are provided in [Figure 3-5](#). In comparison to the stress-strain data given in [Figure 3-4](#), the TC-2 data show a marked decrease in the ductility of the steel. Data for only the lower

three target strains are plotted, as fracture occurred prior to reaching the higher target strains. As shown in [Figure 3-5](#), necking commences at approximately 9 percent strain with fracture at 11 percent strain.

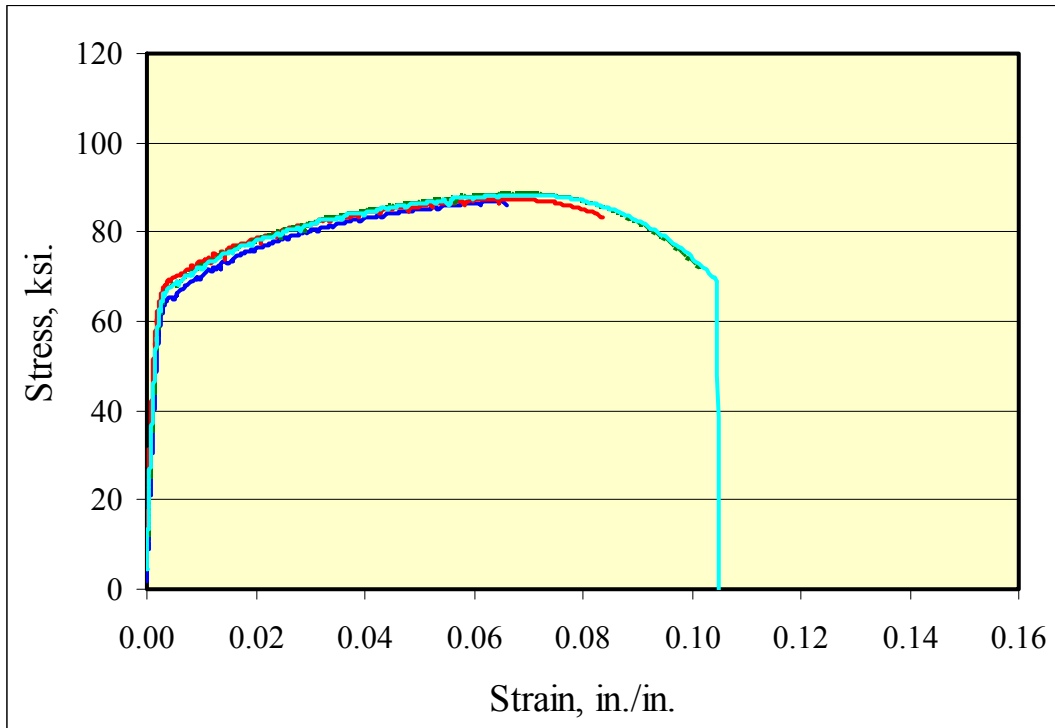


Figure 3-5. Stress-Strain Data for Temperature Condition 2.

[Figure 3-6](#) shows the set of specimens for TC-2, grouped according to the five target strains. Necking can be seen in all three specimens for the target strain of 9 percent. Fracture occurred on the specimens for the target strain of 11 percent. All three specimens fractured prior to reaching their target strain of 13 percent. Only one specimen was tested for the target strain of 1 percent, as it became evident that the steel’s ductility had been substantially reduced and that level of strain could not be achieved.

[Figure 3-7](#) compares the stress-strain plots of a TC-1 specimen strained to 15 percent and a TC-2 specimen strained to 11 percent. Necking began at 14 percent strain for the TC-1 specimen, but little reduction in cross-sectional area occurred. For the TC-2 specimen, necking began at 7 percent strain, with fracture of the cross section at 10.5 percent strain.

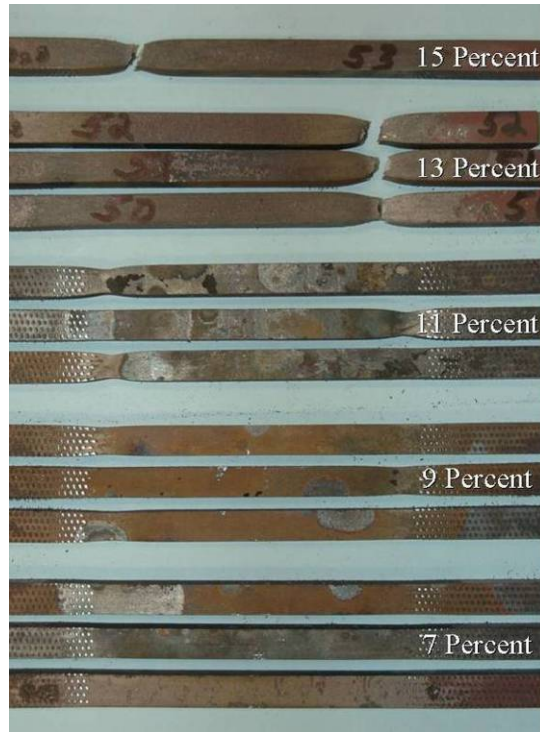


Figure 3-6. Specimen Set for Temperature Condition 2 (Heated to 1150°F, Tested at Approximately 450°F).

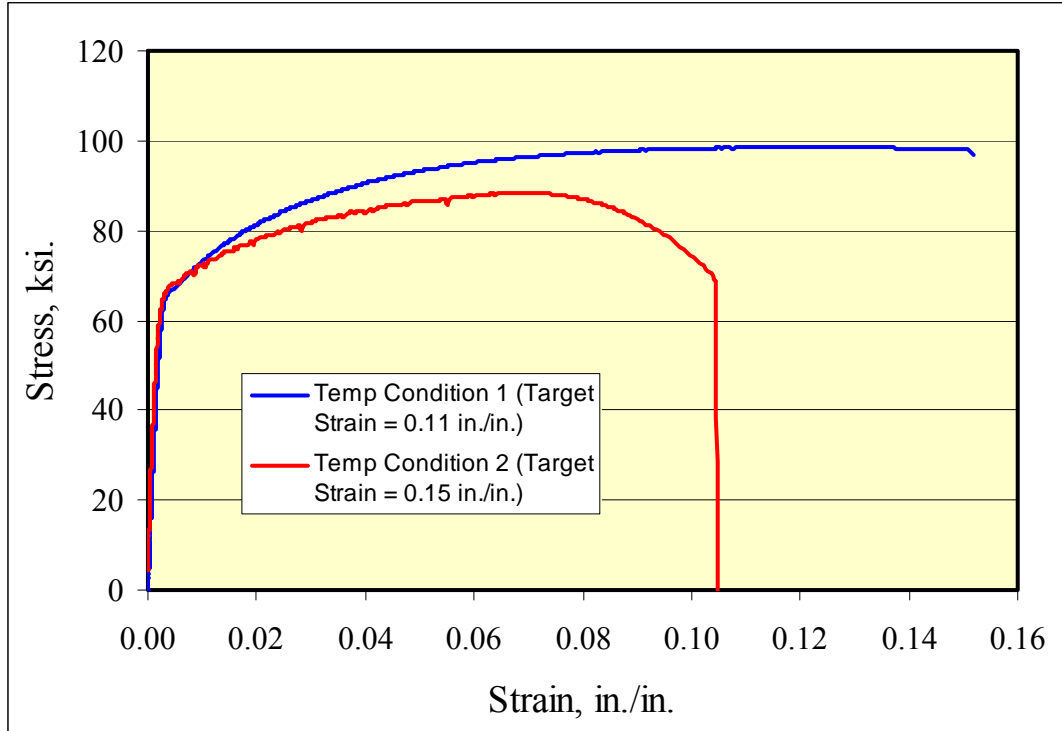


Figure 3-7. Comparison of TC-1 Specimen at 15 Percent Strain and TC-2 Specimen at 11 Percent Strain.

3.3.3 Temperature Condition 3 (TC-3)

The results from the stress-strain data for TC-3 (specimens heated to 1150°F, tested at 1150°F) are provided in Figure 3-8. The stress-strain plots show a significant reduction in both strength and ductility. None of the specimens tested was able to reach its target strain. The yield strength is reduced by an average of 35 percent. The onset of necking occurred at a strain level no greater than 0.5 percent. This strain level resulted in a significant reduction in ductility and is a primary reason why cracking may occur in the plate during the bending operation.

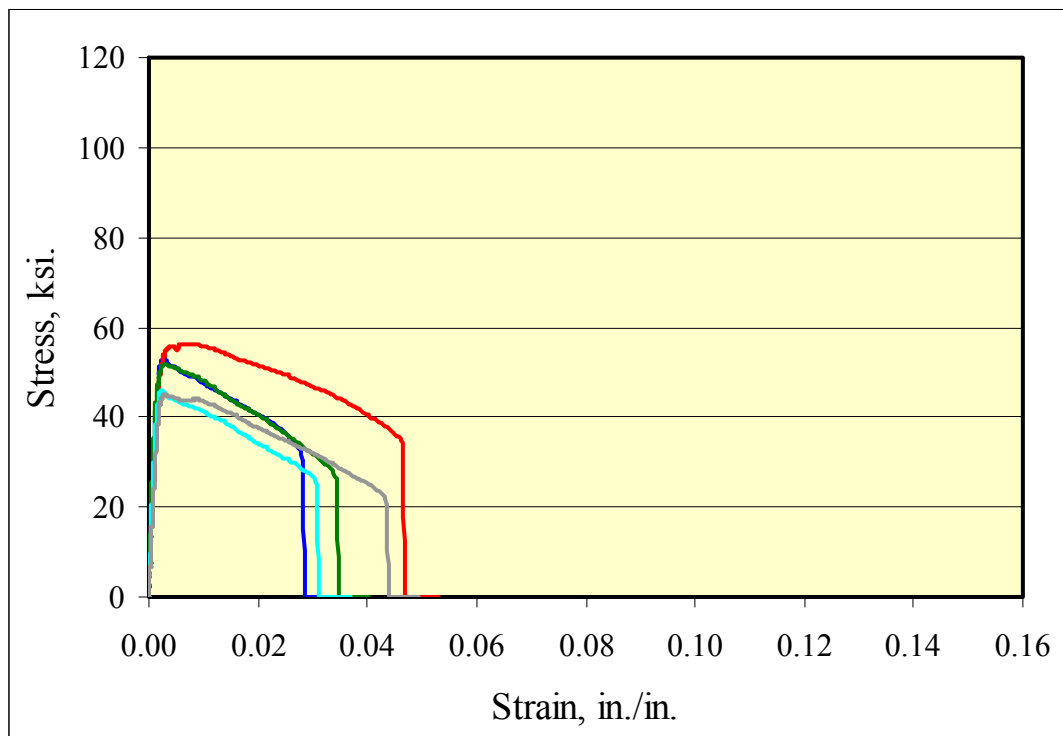


Figure 3-8. Stress-Strain Data for Temperature Condition 3.

3.3.4 Temperature Condition 4 (TC-4)

The results for the stress-strain data for TC-4 (specimens heated to 1150°F, air-cooled to room temperature for testing) are provided in Figure 3-9. The tested specimens that comprised this set are shown in Figure 3-10. Visually, there is no evidence of necking. The stress-strain plots of Figure 3-10 are similar to those of Figure 3-4 with one major exception: the existence of a well-defined yield plateau for the TC-4 specimens. All specimens were able to reach their

target strains. This is evident in [Figure 3-11](#), which compares 15 percent target strain specimens for both temperature conditions. Note that with the emergence of the yield plateau there is a slight reduction in the yield strength.

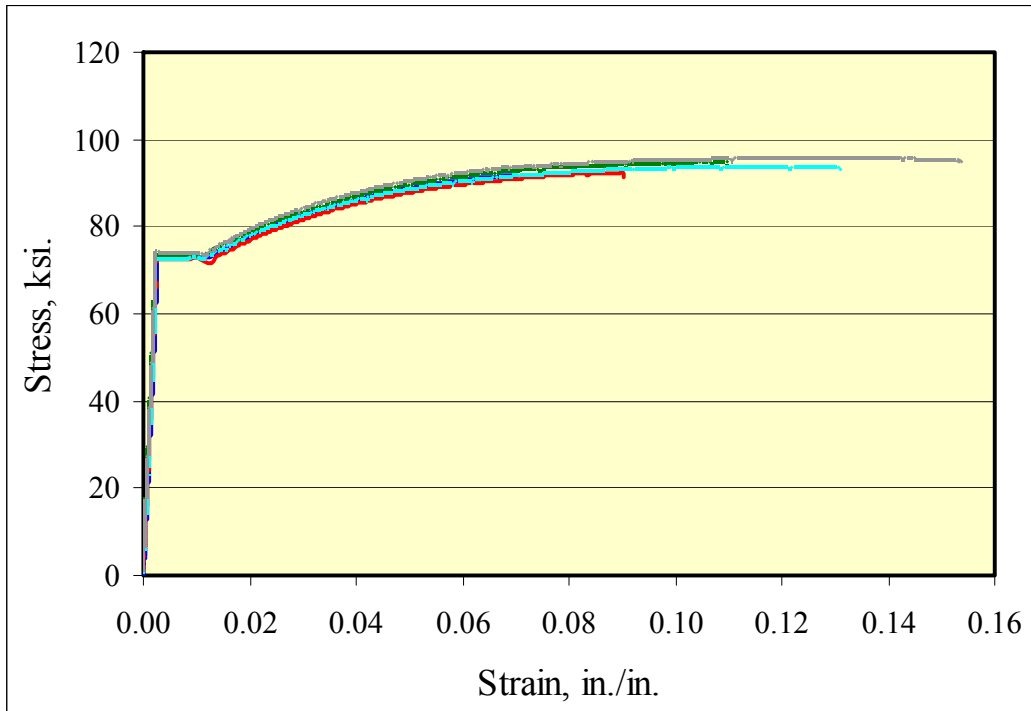


Figure 3-9. Stress-Strain Data for Temperature Condition 4.

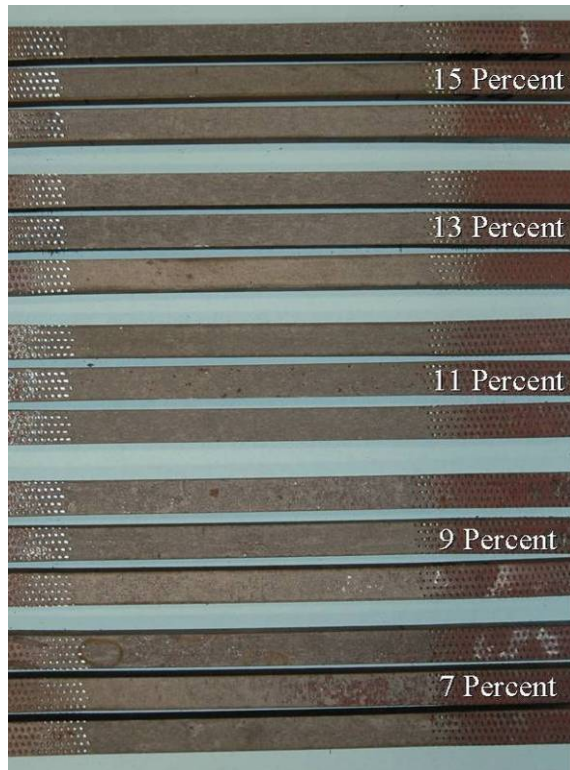


Figure 3-10. Specimen Set for Temperature Condition 4 (Heated to 1150°F, Air-Cooled to Room Temperature and Tested).

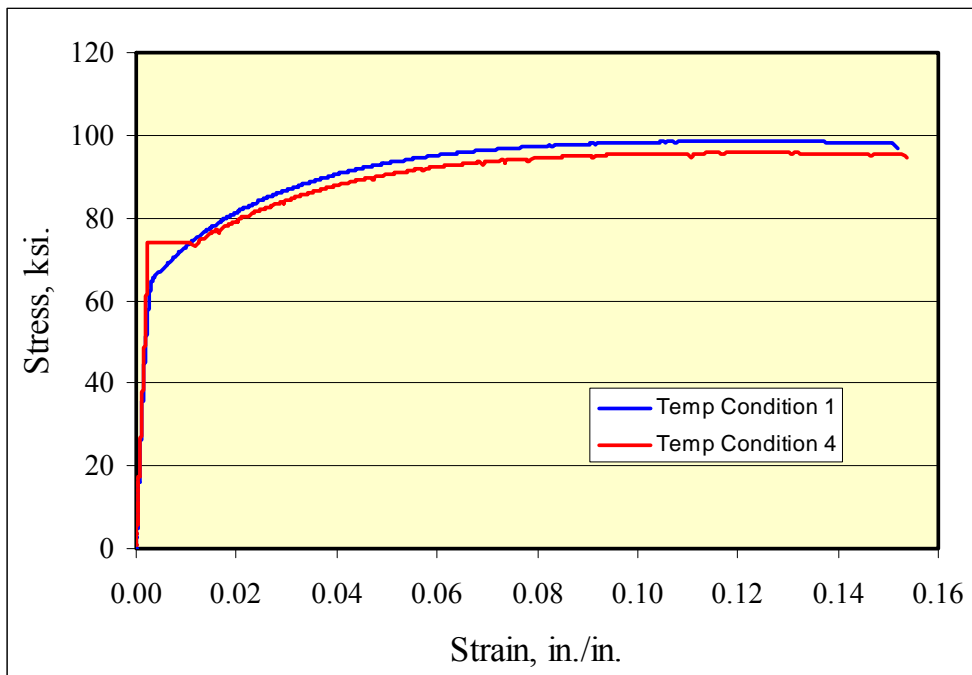


Figure 3-11. Comparison between Temperature Condition 1 and Temperature Condition 4 for a Target Strain of 15 Percent.

3.3.5 Temperature Condition 5 (TC-5)

The results for the stress-strain data for TC-5 (specimens cooled to 0°F, tested while warming) are provided in Figure 3-12. The tested specimens that comprised this set are shown in Figure 3-13. These stress-strain curves are similar to those of TC-1. However, not shown in Figure 3-12 are the stress-strain curves for two specimens of the TC-5 set that necked and fractured prior to reaching their target strains of 11 and 15 percent. These specimens can be seen in the photograph of the complete set of specimens for TC-5 (Figure 3-13) and are plotted in Figure 3-14. The fracture of these two specimens indicates reduced ductility, in addition to fracture toughness, at lower temperatures. Plate bending at reduced temperatures could lead to cracking problems in addition to those associated with the application of heat.

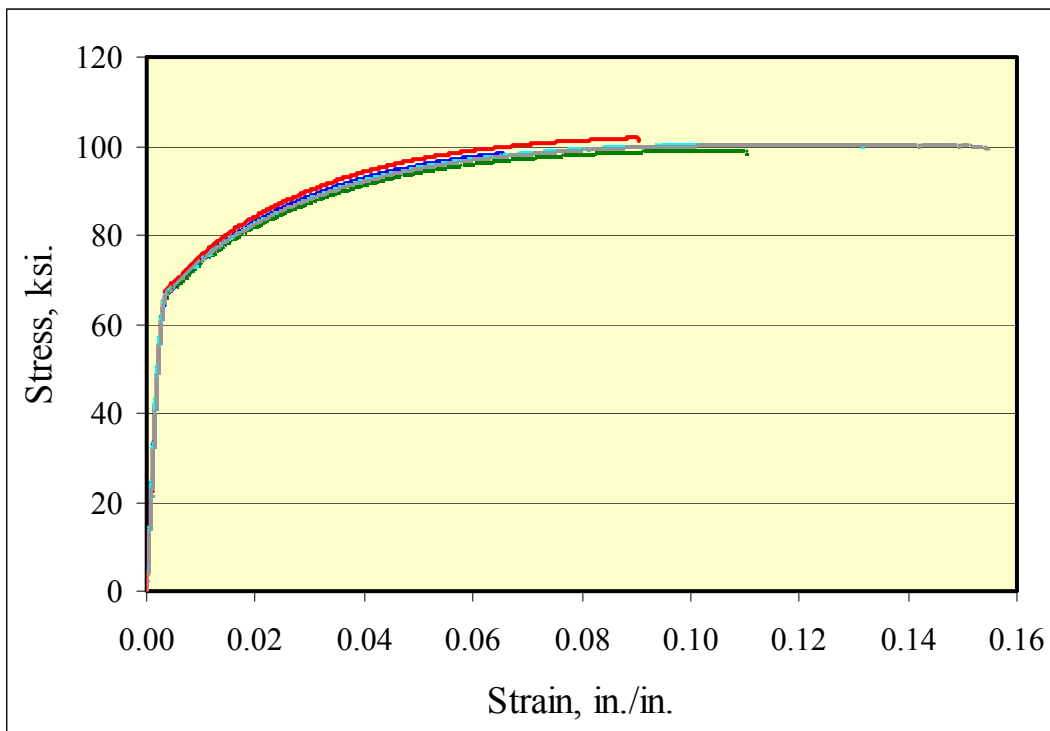


Figure 3-12. Stress-Strain Data for Temperature Condition 5.

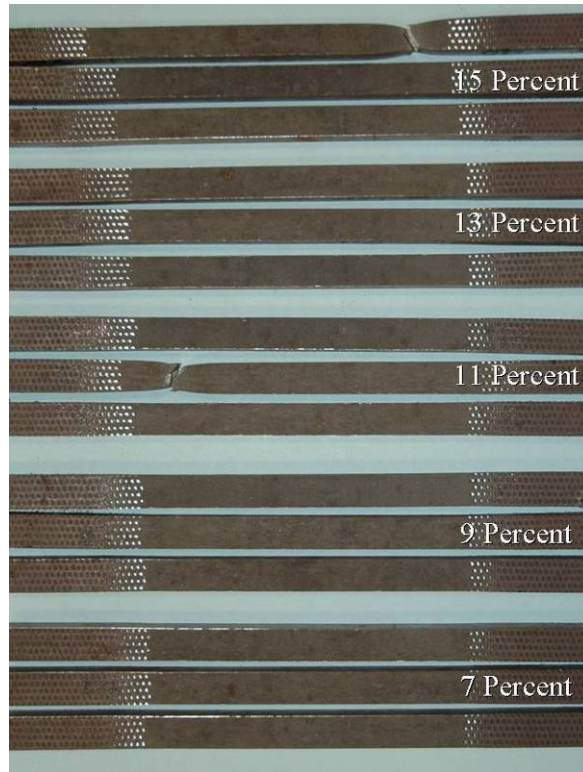


Figure 3-13. Specimen Set for Temperature Condition 5 (Cooled to 0°F, Tested while Warming).

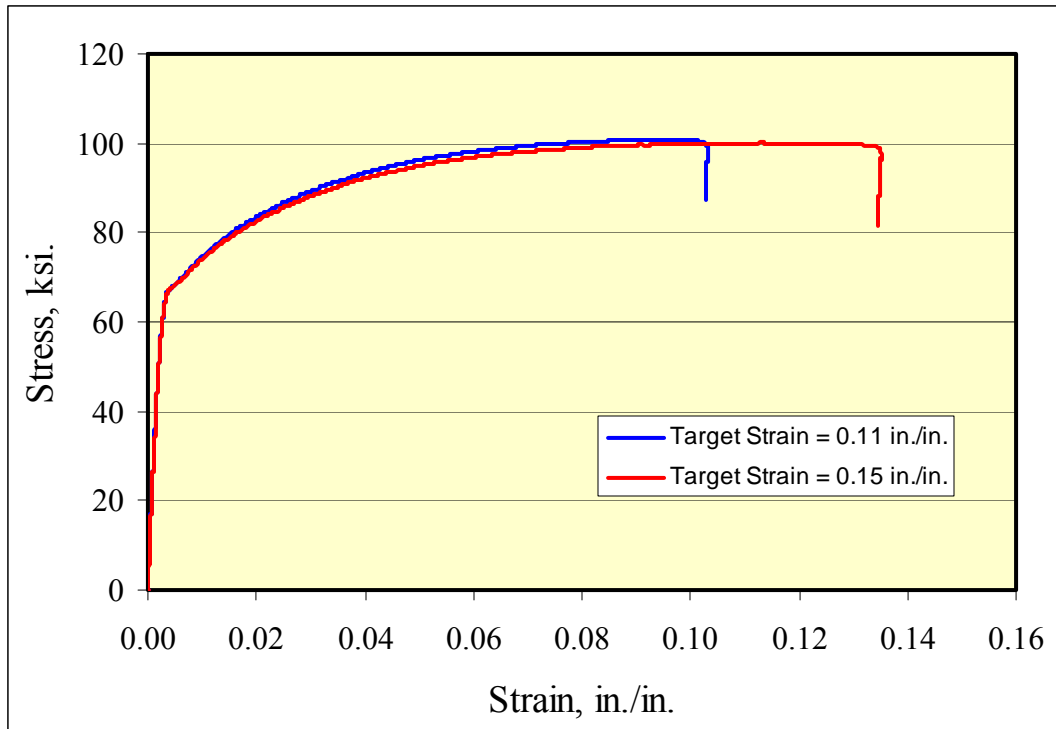


Figure 3-14. Comparison of Stress-Strain Curves for Two Specimens That Fractured Prior to Reaching Target Strain (TC-5).

3.3.6 Fracture Toughness Investigation

CVN specimens were machined from many of the tested tensile specimens in order to investigate the effect of high strain levels on the fracture toughness of the steel plate. Standard specimens were obtained so that the notch of the CVN specimen was located within the gauge length of the tensile specimens and at least 0.75 inches from the gripped region. Also, the CVN specimen did not contain a region of necking. These specifications precluded obtaining CVN specimens from those tensile specimens that experience necking or fracture.

Figure 3-14 shows the CVN test results from a set of specimens for TC-1. As indicated by the data, the fracture toughness decreased as target strains increased. This would be expected, as the ductility of steel decreases with increased inelastic strain levels. Figure 3-15 provides a comparison of data between CVN specimens from TC-1 and TC-4. As shown, fracture toughness is improved by the heating process.

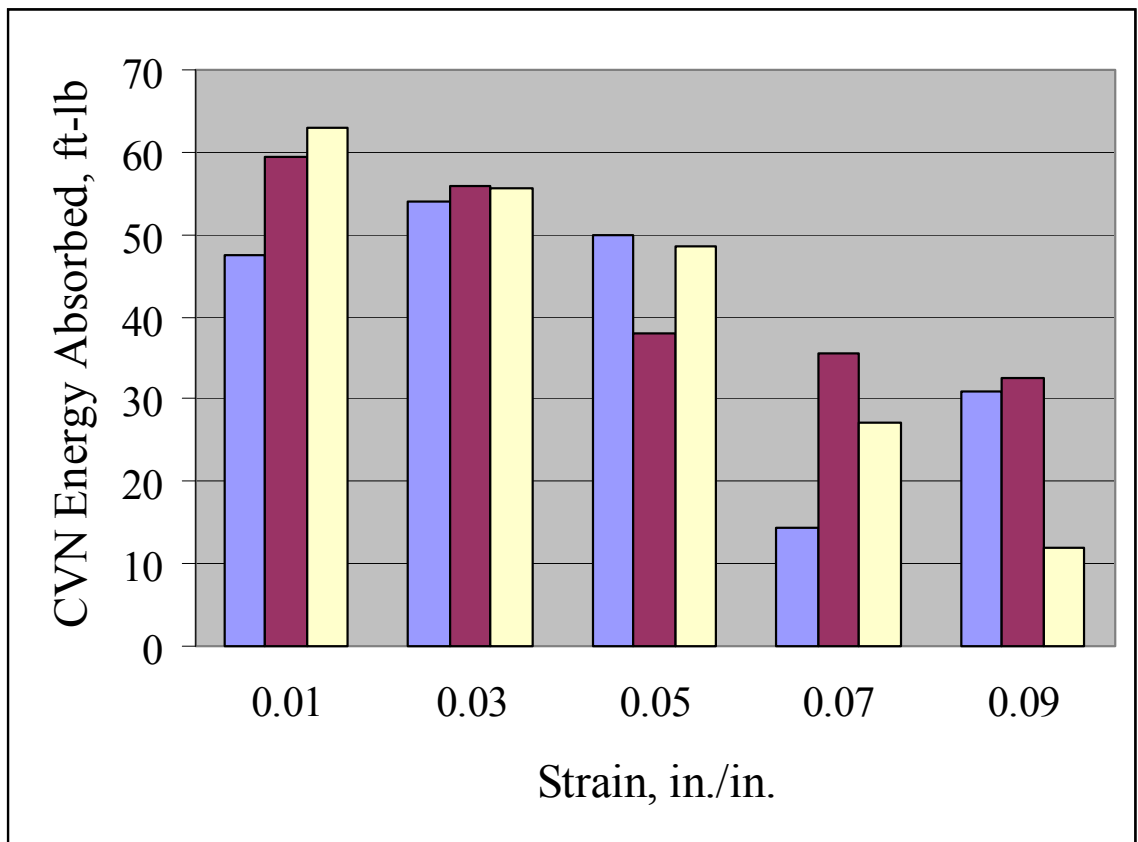


Figure 3-15. CVN Test Data for Temperature Condition 1.

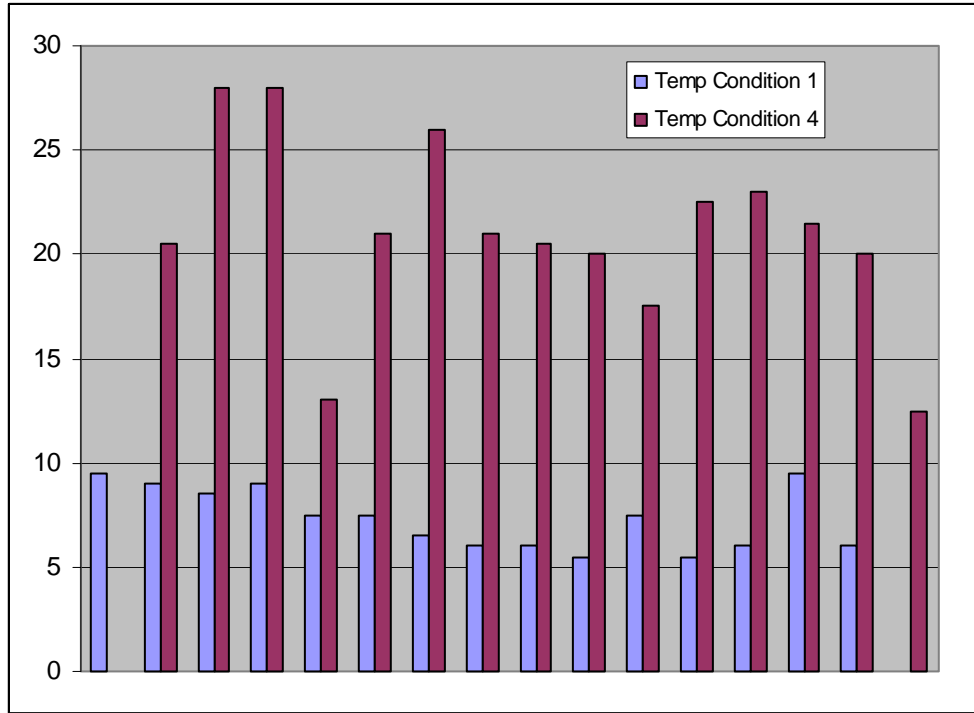


Figure 3-16. Comparison of CVN Test Data between Temperature Condition 1 and Temperature Condition 4.

3.4 CONCLUSIONS AND RECOMMENDATIONS

For the experimental study involving the testing of small-scale tensile specimens, the following observations can be made:

- Typical bending operations significantly over-strain the flange plate.
- Cold-bending is preferred to heat-assisted bending.
- Heat-assisted bending results in reduced ductility (approximately 5 ft-lb).
- The strains should be limited to 0.10 in./in. or 10 percent.

It is clear from the results that a typical bending operation used in the fabrication of highway plate girders results in high levels of strain occurring in the extreme fibers at the point of maximum curvature.

CHAPTER 4: FINITE ELEMENT STUDY

4.1 GENERAL

The experimental program for the plate bending study focused on the strain behavior of small tensile specimens. In order to extend those findings to full-scale behavior, researchers conducted a finite element study.

4.2 APPROACH TO DEVELOPING THE FINITE ELEMENT MODELS

The fabrication of dapped girders often necessitates the application of heat while bending the flange plate. This need arises from the prohibition of cold-bending flanges of fracture-critical members as well as limiting capacities of bending equipment of a particular fabricator. Consequently, it is important to investigate the effects of elevated temperatures and through-thickness temperature gradients on the initial and residual stress distributions as well as the strains that occur at the extreme fibers of the plate. To fully investigate the effects of heat, two finite element models were developed. One model investigated the thermal characteristics of steel, while a second model investigated the mechanical behavior during the bending process. Two different heating methods were modeled to depict the two most common methods used in the fabrication process. One thermal model modeled the temperature distributions resulting from heating a steel plate in a furnace to a uniform temperature and then allowing natural convection to take place. The other thermal model depicted the use of an acetylene torch for heating the plate to an appropriate surface temperature. The thermal models were solved first. The resulting temperatures were then imported into the structural model to determine the stresses resulting from temperature and the bending process.

The mechanical properties of steel vary greatly as temperature increases. Because of this fact, several researchers have proposed various methods of determining stress-strain curves when there is a lack of experimental data. Some of the research and proposed methods include work by Poh, Lie, and Eurocode 3 (Poh 2001, Lie 1992). Researchers compared these methods and found that the Poh stress-strain equation models the linearly elastic region, plastic plateau, and the strain-hardening portion of the stress-strain curve in just one equation. Doing so allows for ease in using computer programs for plotting the different stress-strain-temperature curves that would

be used in the structural model. A more detailed discussion on the analysis and comparison of the different stress-strain-temperature curves is given in [Christian \(2005\)](#).

4.3 CONVECTION MODEL

Several assumptions were made for modeling the plate during cooling. The first assumption was that the plate would not be cooled by forced convection but rather by natural convection and radiation. This assumption was made because in practice only natural convection is allowed until the plate is cooled below 600°F and then cooling can only be aided by dry compressed air ([AASHTO/NSBA 2002](#)). Another assumption was that the air temperature during cooling would be 80°F. In reality, the air temperature varies depending on the climate in which the fabrication plant is located. The steel's thermal properties were assumed to be those of typical structural steel with a thermal conductivity of $28.7 \frac{Btu}{hr \cdot ft \cdot ^\circ F}$ and a coefficient of heat

transfer of $11.01 \frac{Btu}{hr \cdot ft^2 \cdot ^\circ F}$.

The steel plate that was modeled was assumed to be simply supported with its dimensions 40 inches long and 6 inches wide. Therefore, internal stresses would not develop during cooling from support fixity. Different plate thicknesses were modeled to look at various temperature gradients that might occur during fabrication of flange plate. [Figure 4-1](#) shows a typical representation of the thermal model and where the natural convection boundaries occurred. Quad 8 Node elements that were 0.2 inches square were used. Considering the elements as Quad 8 Node located a node every 0.10 inch along the model's faces so that the results would be more accurate than just a four-noded element that would only determine results every 0.2 inches. It was assumed that the convection boundaries would occur only on the top and bottom surfaces of the plate, based on the assumption that during fabrication the heated plate is at least several feet long and the bending occurs at a location where there is little effect on the plate's end convection.

Preliminary finite element analysis was performed to investigate whether convection occurring at the ends of the plate influences the results toward the inner length of the plate where the bending takes place. This investigation showed that end convection only affected the

through-thickness temperature gradient within a few inches of the plate end and could therefore be ignored. Subsequent temperature modeling ignored end convection altogether.

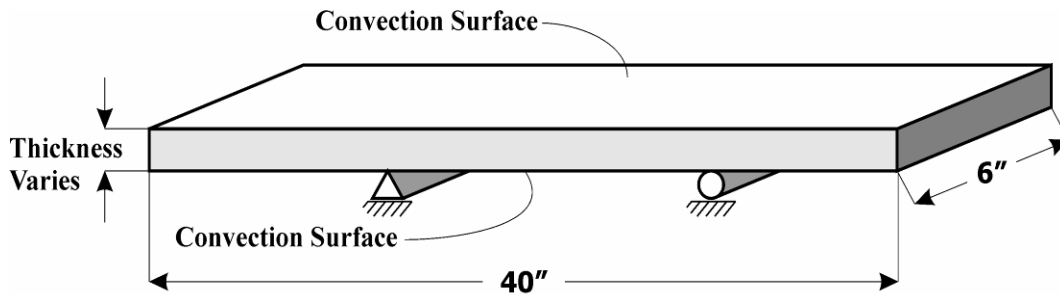


Figure 4-1. Convection Model.

The model simulated what occurs after a plate is taken out of a furnace after a uniform temperature is achieved and then is allowed to naturally air cool. It was assumed that at the time the plate was removed from the furnace, the plate had reached a uniform temperature of 1100°F. Temperature readings were taken after 5 and 10 minutes of air-cooling. These times were selected to represent the time it would take for the plate to go from the furnace to the bend press and to induce the proper bend. The temperature readings were later introduced into the structural model to simulate bending at elevated temperatures.

4.4 CONDUCTION MODEL

In practice, some fabrication methods use acetylene torches to heat the steel to desired temperatures prior to bending (Figure 4-2). The acetylene torch heats the steel from the outside in so that the plate's surface is hotter than the inside of the plate. Because of this, the plate's behavior during bending could be different from the furnace heating method.

The steel's thermal conductivity was modeled as $28.7 \frac{Btu}{hr \cdot ft \cdot ^\circ F}$ with the plate's initial temperature assumed to be a uniform 80°F. The temperature of 1200°F that the plate was allowed to reach was found in section 5.1 of the AASHTO/NSBA steel bridge fabrication guide specification S2.1-2002 (AASHTO/NSBA 2002). Because of this limit, the conduction model was only allowed to achieve 1200°F on the plate's surface before the heat source was removed. FHWA suggested a method of applying heat to a plate that is more than 1 inch thick using a

rosebud tip ([FHWA 1998](#)). There is no clear heating rate specified in codes; different fabricators run the rosebud at different gas pressures and in different climatic conditions. Some manufacturers choose to use propane instead of acetylene to heat the plate before bending because propane is a safer gas to use and store. However, propane does not heat steel as quickly as acetylene does. For this reason, only the maximum temperature the plate can achieve at the end of the heating process is regulated. As the heating rate increases, so does the temperature gradient through the plate's thickness. [Figure 4-3](#) shows modeling of different heating rates for a 2-inch thick plate and shows the resulting temperature gradients.



Figure 4-2. Acetylene Torch Heating.

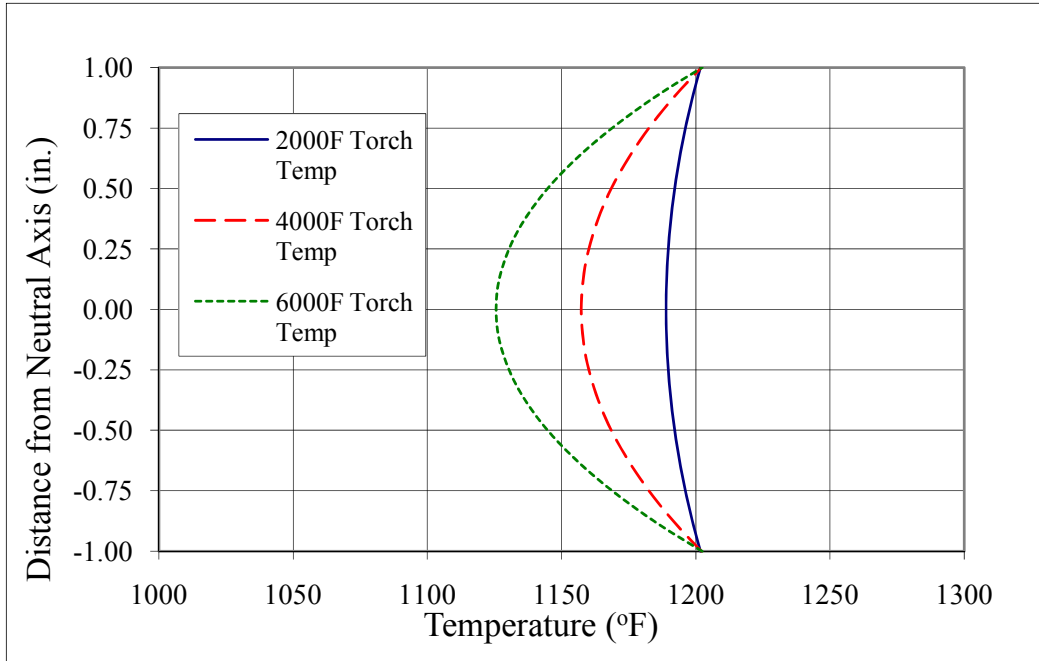


Figure 4-3. Comparing Heating Temperatures for 2-Inch Plate.

Because there is no significant difference in the temperature gradient with the different heating rates, all three heating rates were investigated by subjecting the model to a single-point bend and comparing the resulting through-thickness stress distribution. The difference in stresses resulting from this comparison was insignificant, as shown in Figure 4-4. Therefore, researchers decided that 4000°F would be a close approximation to the torch’s heating temperature during the fabrication of the flange plates. The small variation at each temperature in the steel’s through-thickness stresses can be explained by examining the steel’s stress-strain curve. As the steel increases in temperature, the slope of the curve in the plastic region becomes very small and closely resembles a bilinear curve. For this reason the steel, after yielding, will remain at a constant stress and will be unable to carry more load. Additional loading will have to be carried by material that has not yet yielded. Without consideration of thermal expansion, the tensile and compression surfaces of the plate are equal in magnitude. With the introduction of thermal expansion during elastic loading, the compression surface will be greater in magnitude than the tensile surface. As the bend becomes more severe, the stress at the mid-span of the plate starts to resemble a perfectly plastic stress distribution that cancels out any effect of the steel’s coefficient of thermal expansion. Since the flange plate may be bent at sharp bends and at high

temperatures, the effect of the steel's coefficient of thermal expansion is very small during the bending process.

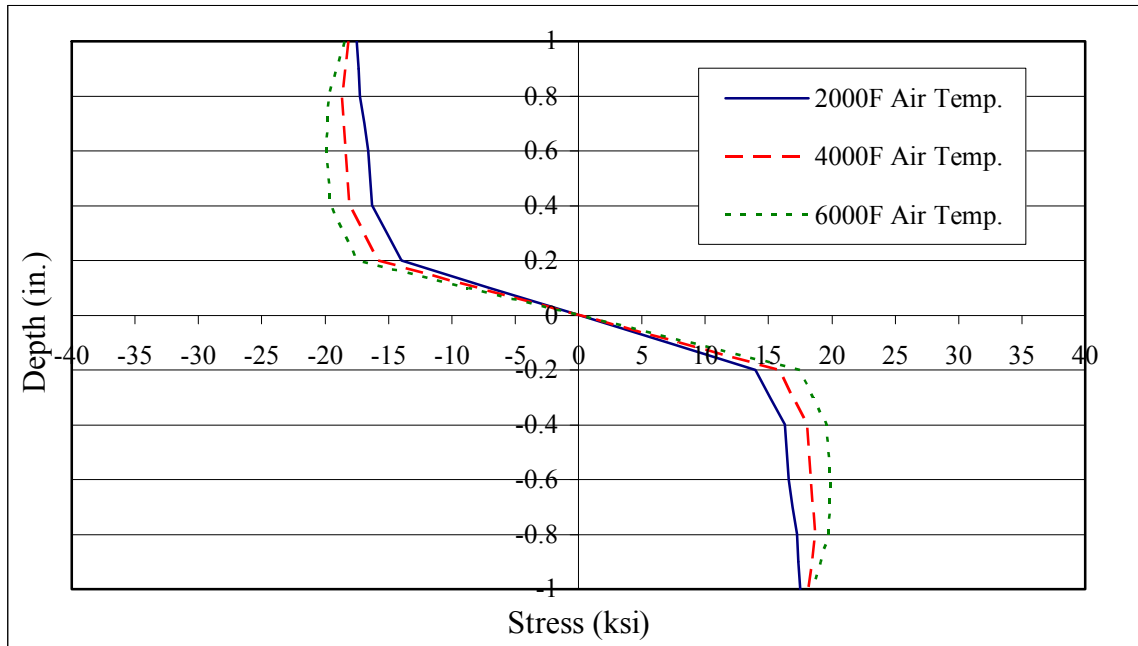


Figure 4-4. Comparing Through-Thickness Stresses.

For investigating convection effects, the steel was allowed to absorb heat through conduction boundaries along the plate's surface (Figure 4-5). To further model the heat that is generated by a rosebud's tip, the temperature of the air above and below the top and bottom surfaces of the plate was at 4000°F simultaneously until the surface of the plate reached a temperature of 1200°F. The plate's dimensions were assumed to be the same as the plate that was modeled undergoing convection in the previous section.

The assumption that the plate is heated across its entire surface is a simplification of the torch heating process. In reality, the plate will only be heated in the region where the bend is to occur. But with the assumptions that bending occurs immediately after heating is completed with no convection allowed to take place and that the fabricator will heat an area of 2 inches on either side of the bend location prior to bending, the fabrication process is accurately depicted. The assumptions had little effect on the resulting stress and strain distributions. Heating the flange plate 2 inches on either side of the bend will later be shown to cause all of the resulting stress and

strain distributions to occur in the heat-affected region so little effect of the unheated plate will be present.

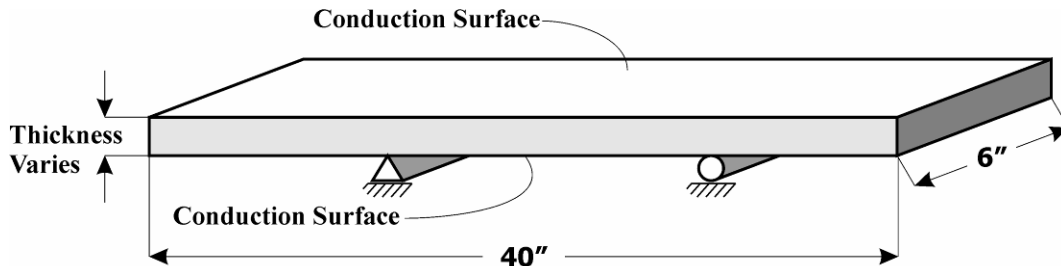


Figure 4-5. Conduction Model.

4.5 STRUCTURAL MODEL

Once the temperature effects were determined, the temperature values were imported into the structural model so that the model could be bent at elevated temperatures. The structural model had the same dimensions as that of the thermal model with a line load located at the center of the plate, as shown in [Figure 4-6](#).

The model was assumed to undergo plane strain with the stress-strain curves varying according to the temperature at various nodes. The stress-strain curves were input into the model as multi-linear curves. This is a valid representation of the stress-strain curve because as a curve is divided into small enough pieces it can be accurately represented by a collection of straight lines. When dividing the stress-strain curve up into parts for use in the multi-linear option in ANSYS 8.0, the slope of all lines must always be positive. It was determined that if the model's temperature was between two stress-strain curves, ANSYS 8.0 interpolated between the two curves to obtain a new stress-strain curve for that specific temperature. The coefficient of thermal expansion for steel was also added into the material properties so that the stresses caused by the difference in temperature could be added to the overall stress that the plate would undergo. The structural model was modeled with 0.2-inch square Quad 8 Node 82 elements so that the results would be determined every 0.1 inch along the element's faces. Using these nodes instead of a four-noded element allowed more accurate results.

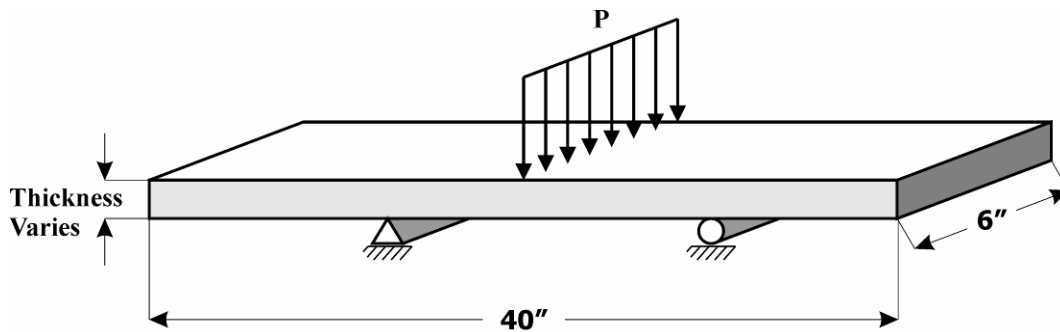


Figure 4-6. Structural Model.

A convergence test was performed on the structural model in order to determine if the model was refined enough or if elements needed to be added to achieve the desired accuracy. The model was run with three different element sizes of 0.2-, 0.14-, and 0.1-inch squares over the entire span of a 10-inch plate. The results of the convergence test indicated the 0.2-inch square mesh size was adequate for use with the structural model. A detailed discussion of the convergence test and its results can be found in [Christian \(2005\)](#).

4.6 THERMAL RESULTS

4.6.1 Through-Thickness Temperature Gradients after Furnace Heating

Using plate thicknesses of 1, 1.5, and 2 inches, which are common in fabrication of bridge girders, a plate was simulated to undergo air-cooling once it was removed from a furnace after reaching a uniform temperature of 1100°F. Through-thickness temperatures were determined for simulated air-cooling periods of 5 and 10 minutes.

Five and ten minute temperature distributions were plotted at the plate's midspan for 1-, 1.5-, and 2-inch thick plates. For the 1-inch thick plate, the surface temperature cooled to 803°F after 5 minutes and 565°F after 10 minutes. The difference in the surface temperature and the plate's mid-thickness was 5.5°F after 5 minutes of cooling and 4°F after 10 minutes of cooling, as shown in [Figure 4-7](#). The small through-thickness temperature gradient can be attributed to the relatively thin plate thickness.

The 1.5-inch thick plate surface temperature cooled to 885°F after 5 minutes and 691°F after 10 minutes. The difference in the surface temperature and the plate's mid-thickness was

found to be 9°F after 5 minutes of cooling and 7.5°F after 10 minutes of cooling. As shown in [Figure 4-8](#), the surface temperature decreased 194°F after 10 minutes of cooling from the temperature measured after 5 minutes of cooling (885°F). This temperature decrease plays an important role in the amount of residual stresses that will form as result of bending because the mechanical properties of the steel increase as the temperature decreases.

For the 2-inch plate thickness, temperature gradients of 13°F occurred after 5 minutes of air-cooling and 12°F after 10 minutes of air-cooling ([Figure 4-9](#)). The surface temperature cooled to 937°F after 5 minutes and 794°F after 10 minutes.

In all the plate sizes investigated, the change in the temperature gradient for 5 and 10 minutes of air-cooling was small. However, there is a large difference in surface temperatures at which the plate will undergo the bending process for the various plate thicknesses. Because the plate cools down from an 1100°F uniform temperature, the resulting residual stress and strain distributions will be affected.

The temperature gradients resulting from air-cooling the plate for 5 and 10 minutes were imported into the structural model to simulate the bending of a plate after it has undergone furnace heating.

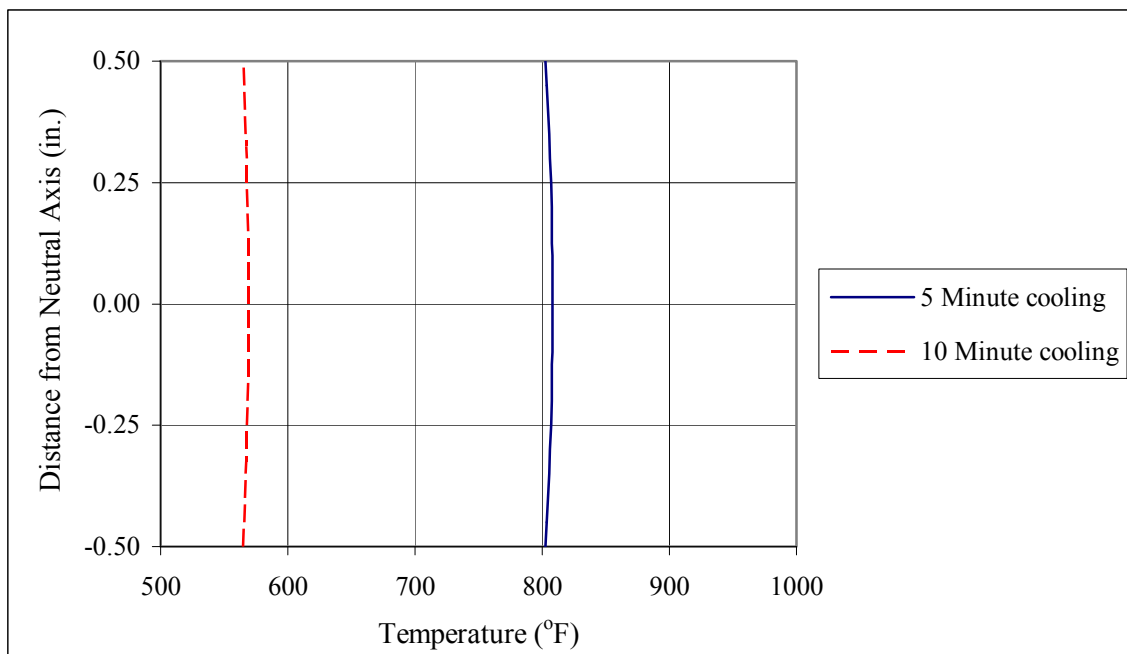


Figure 4-7. Through-Thickness Temperature Distribution for 1-Inch Plate.

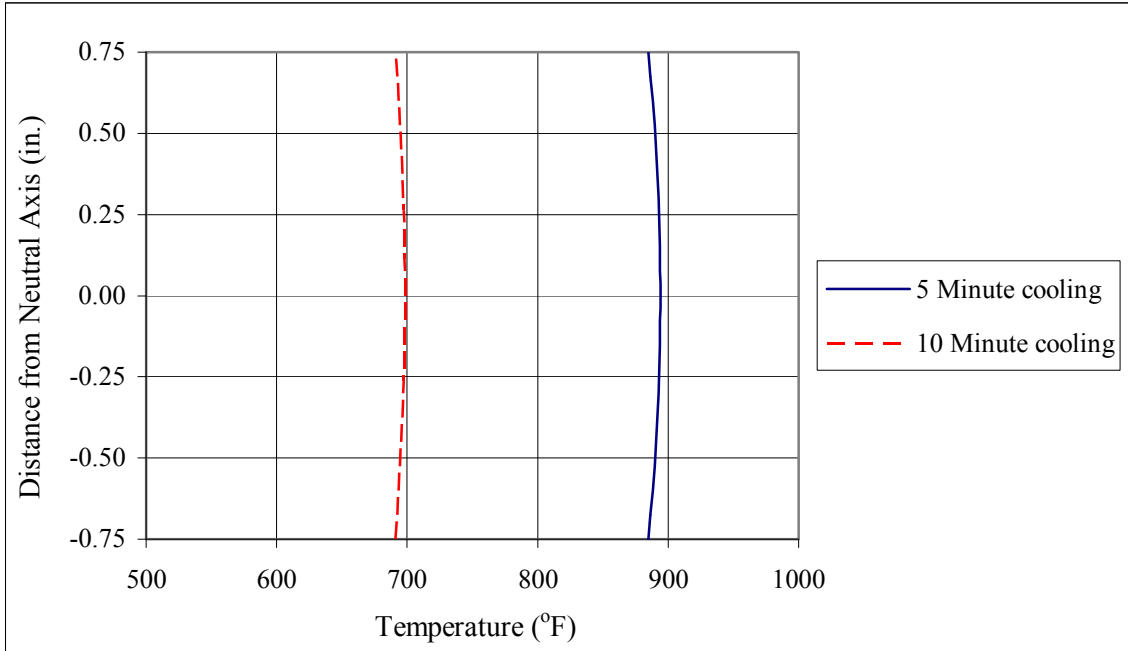


Figure 4-8. Through-Thickness Temperature Distribution for 1.5-Inch Plate.

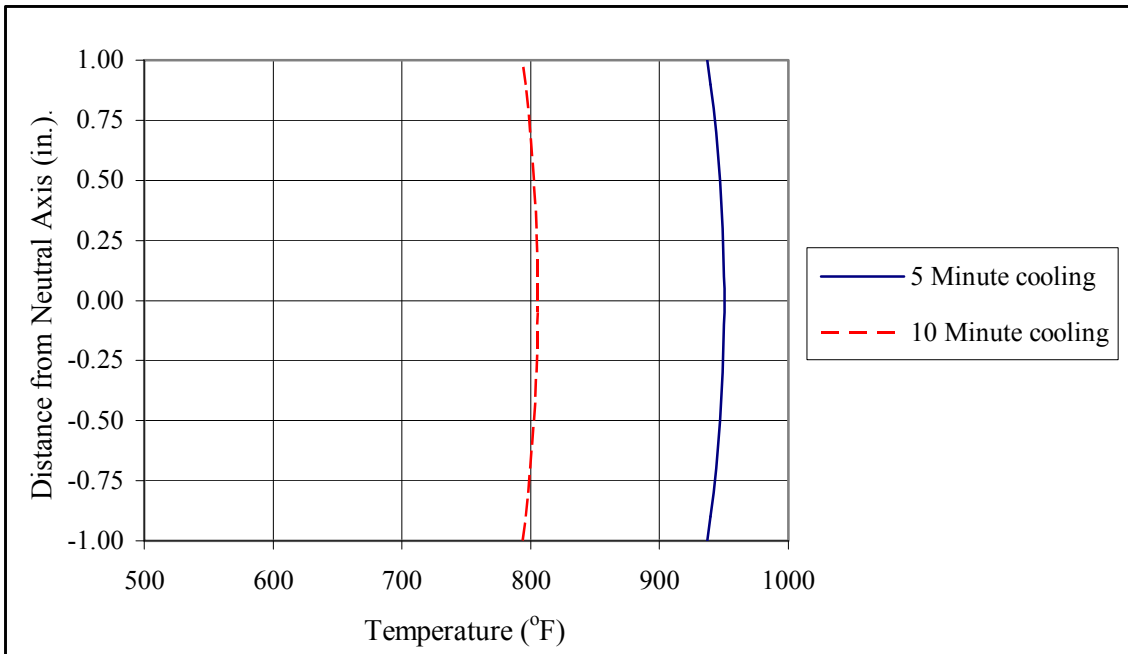


Figure 4-9. Through-Thickness Temperature Distribution for 2-Inch Plate.

4.6.2 Acetylene Torch Temperature Gradients

In addition to heating the plate uniformly to 1100°F in a furnace, heating the plate using an acetylene torch was also simulated. This heating method results in a non-uniform temperature

gradient prior to the cool-down period and could therefore exaggerate the final or residual stress or strain distributions. During the heating process, the extreme fibers would be expected to go into compression due to their expansion relative to the inner fibers.

A conduction model was developed and the resulting stress distributions were found for 1-, 1.5-, and 2-inch plates. In general, as the plate increases in thickness, the resulting temperature gradient increases, as well as does the amount of time required for the plate's surface to reach 1200°F. In [Figure 4-10](#), the resulting temperature gradient caused by torch heating is shown for a 2-inch plate. Heating the ends of the plate during torch heating was determined to only affect the temperature gradient within a few inches of the end, and it was determined that bending would not occur in this region during the fabrication of the flange plate.

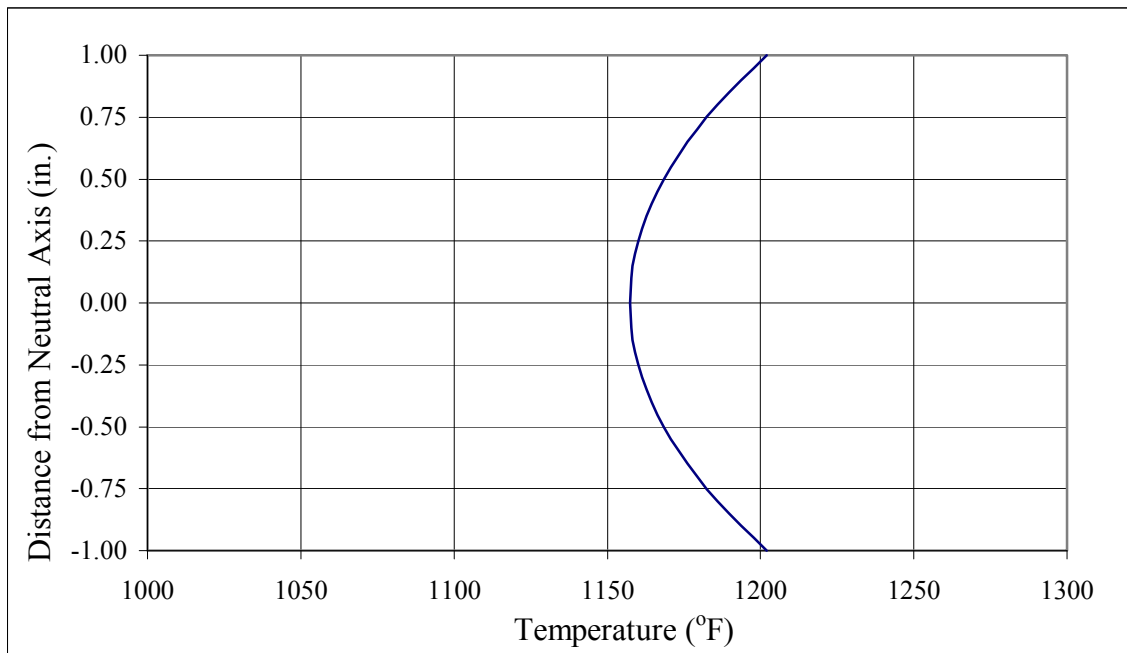


Figure 4-10. 1200°F Surface Temperature 2-Inch Plate.

The time that it took a 1-inch plate to increase from a uniform temperature of 75°F to a surface temperature of 1200°F was 4 minutes and 35 seconds when the air temperature along the top and bottom surface was 4000°F. It was assumed that heating took place simultaneously from both sides of the plate. Therefore, the time is less than that required if a single torch was used to heat the plate. The resulting difference in temperature from the plate's outside surface to its neutral axis, shown in [Figure 4-11](#), was 22°F. The plate surface at the end of the heating process

was 1206°F, 6°F higher than the target surface temperature, but it was decided that 6°F would not significantly affect the bending results.

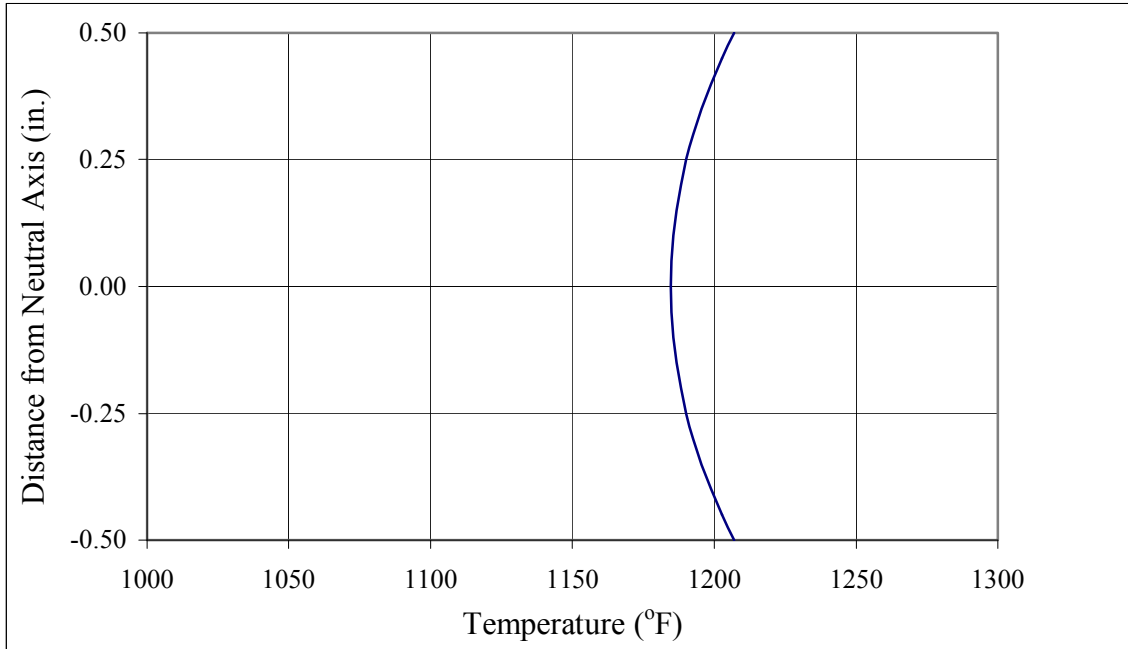


Figure 4-11. Acetylene Torch Through-Thickness Temperature Distribution for 1-Inch Plate.

The 1.5-inch plate had a higher temperature gradient than the 1-inch plate because the heat took longer to flow from the plate's surface to its inner core due to the increased plate thickness. The temperature gradient for a 1.5-inch plate, shown in [Figure 4-12](#), was 34°F, an increase of 10°F from that of the 1-inch plate. The surface temperature of the 1.5-inch plate after the heating process was completed was 1200°F. As the plate thickness further increased to 2 inches, the temperature gradient increased to 44°F, with the amount of time that it took the plate to reach this temperature longer than that required for either the 1-inch or 1.5-inch plate.

The temperature gradients resulting from torch heating were imported into the structural model to simulate the bending of a plate as if it was originally heated by means of a torch.

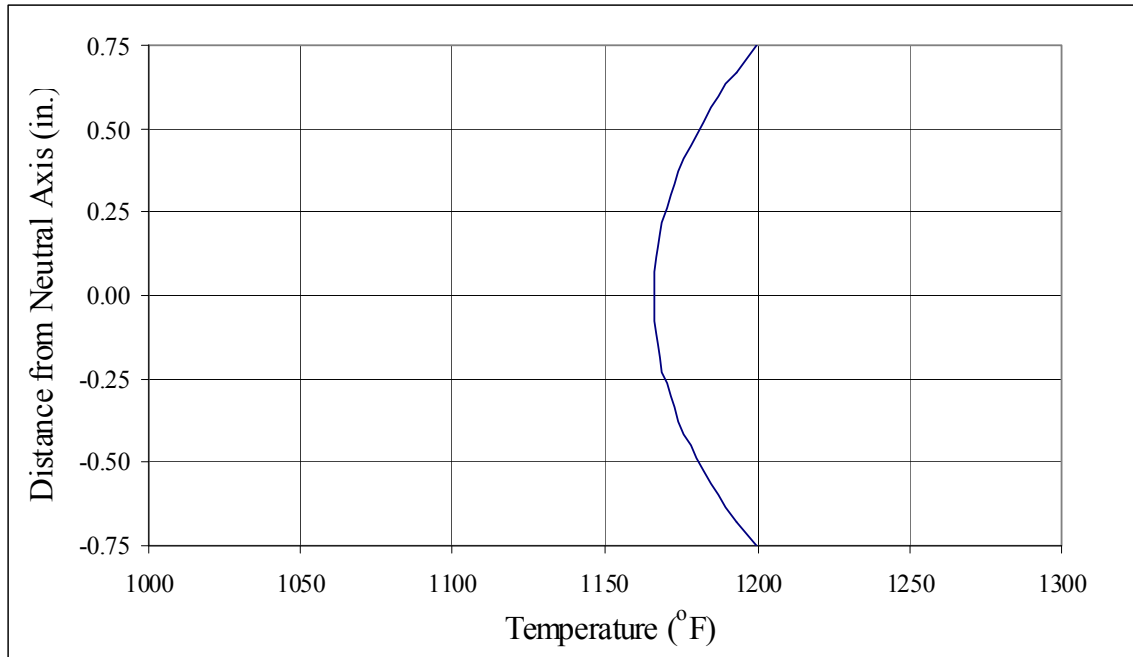


Figure 4-12. Acetylene Torch Through-Thickness Temperature Distribution for 1.5-Inch Plate.

4.6.3 Comparison of Heating Methods

Comparison of the temperature gradients obtained by the two different heating methods showed that the two different heating methods yielded temperature gradients that were opposite each other. The furnace heating method caused the coolest portion of the plate to occur at the plate's surface and heating using a torch caused the coldest region in the plate to occur at the plate's centroid. When a torch was used during the fabrication process, the resulting temperature gradients at the time of bending were greater than those of a plate that underwent furnace heating. If the plate was allowed to cool after heating with an acetylene torch, the temperature gradients in the plate resembled convection gradients. These gradients are a result of steel radiating heat into the air faster than heat can be transmitted through the plate's thickness. When a torch is used to heat the plate to a surface temperature of 1200°F, the temperature at all points in the plate is higher than the initial temperature of the plate that underwent furnace heating, resulting in the plate following a stress-strain curve that is of smaller magnitude to the one that the convection plate follows.

4.6.4 Stress-Strain-Temperature Curves

Highway girders are commonly fabricated using 50 ksi and 70 ksi (grade 50 and 70) structural steel. The mechanical properties of each of these grades of steel change with temperature, and it is important to accurately represent these changes in order to correctly understand what occurs in the material during the different load stages in a bending operation. The equations proposed by Poh (2001) were determined to be the most accurate and conservative representation of the steel's mechanical properties in the absence of available experimental data. Using these equations, stress-strain curves were found for grade 50 steel (Figure 4-13). It was decided that even though ANSYS 8.0 will interpolate between the various stress-strain curves, the equation proposed by Poh would be used to create a series of stress-strain curves in the temperature range under investigation. The same procedure was used to create the 70 ksi stress-strain-temperature curves that are shown in Figure 4-14.

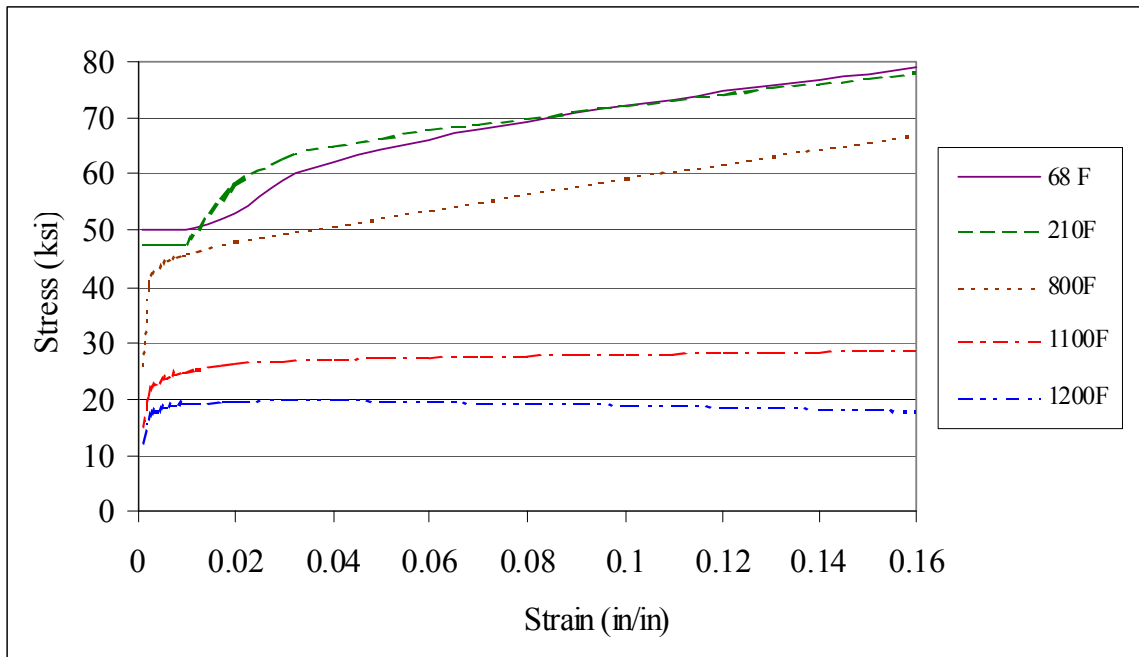


Figure 4-13. Grade 50 Stress-Strain-Temperature Curves.

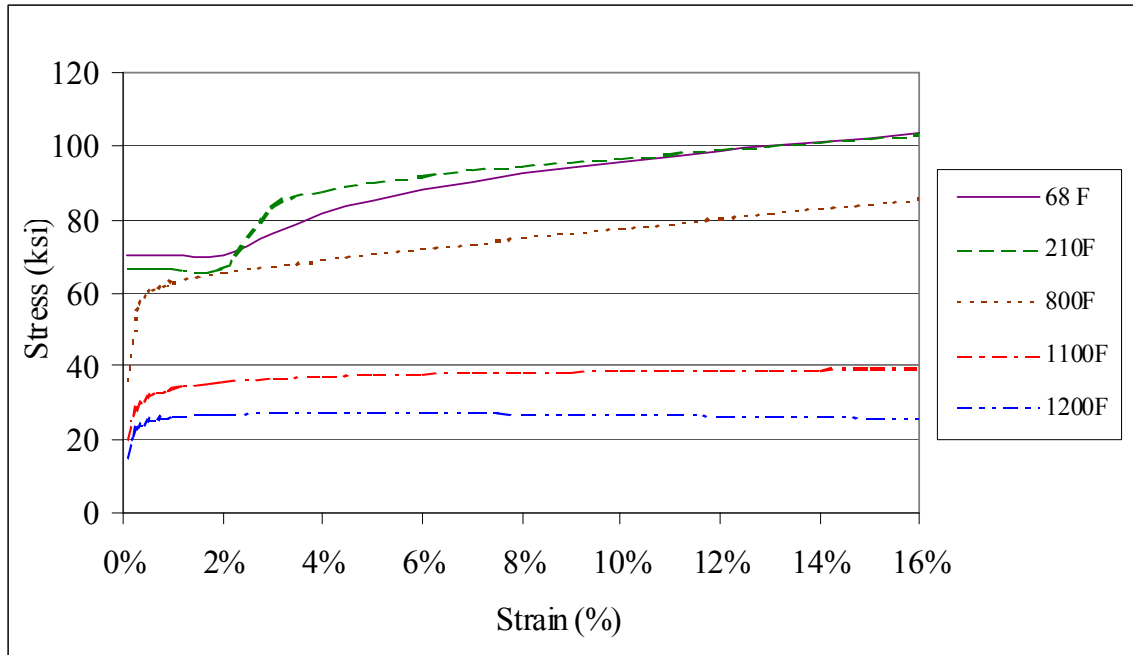


Figure 4-14. Grade 70 Stress-Strain-Temperature Curves.

4.6.5 Six-Inch Radius Bend

In dapped trapezoidal box girder fabrication, a typical radius used to bend the flange plate has been 6 inches. Some fabricators that have used this bend radius experienced crack formation during the bending process. A finite element model was developed to investigate and predict the level of through-thickness residual stresses and strains that formed as a result of the bending process and to determine what effects the application of heat might have on these distributions.

Due to the severity of the strains and the need to achieve a constant 6-inch radius, multiple bend points (hits) must be used. There are no set specifications on exactly how many hits are to be used and how far the hits are to be from one another. It was decided to model the plate as simply supported with a total of five different loadings at 1-inch intervals. As the line load moved across the plate the supports moved with it so that the load would always be applied at the midspan. Since the displacements of a 90-degree bend are so large, only a 4-inch segment of the 6-inch radius was modeled. This was deemed acceptable, for it was observed that during the bending process stresses and strains resulting from the bending remained relatively constant throughout the length of the bend. In [Figure 4-15](#), the bending locations for the first three loadings are shown along with the final step that shows the correct bend radius along a 4-inch segment.

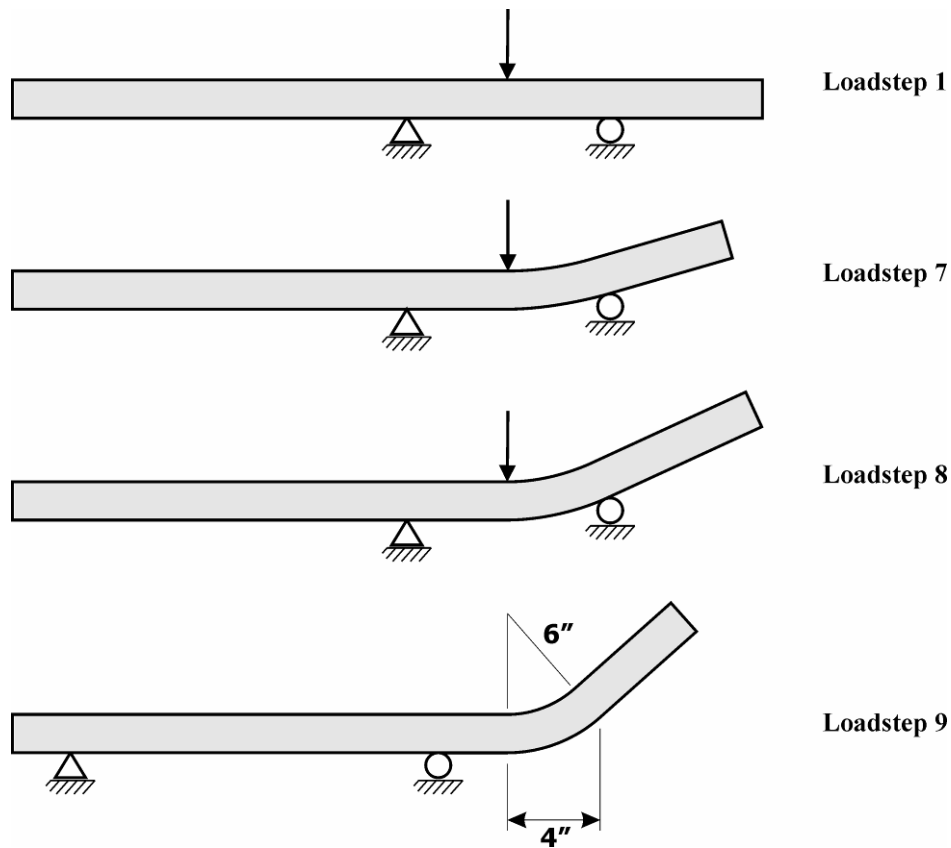


Figure 4-15. Load Steps.

4.6.6 Surface Residual Stress Distribution

The magnitude of surface residual stress that occurs during fabrication of the bent flange is largely influenced by the temperature of the plate at the time of bending. In [Figure 4-16](#), the lowest magnitude of surface residual stresses occurred when the plate was heated using a torch to a surface temperature of 1200°F. The highest magnitude of surface residual stress occurred when the plate was bent at room temperature. These results directly relate to the stress-strain-temperature curves that were developed in [Christian \(2005\)](#); as the temperature increases the amount of stress that can occur in the material decreases. Therefore, the resulting surface residual stress also decreases with respect to temperature. [Figure 4-16](#) also shows that the residual stresses caused by air-cooling the plate for both 5 and 10 minutes substantially increase the amount of surface residual stresses in the plate to nearly the level seen at room temperature bending. This higher magnitude of surface stress developed from air-cooling from the 1100°F

uniform temperature increases the plate's chances of developing cracks. This increase in surface residual stress after 5 and 10 minutes of air cooling can also be seen in the 1.5- and 2-inch plate thicknesses that were studied (Figure 4-17 and Figure 4-18, respectively). As the thickness of the plate increased from 1 inch to 1.5 inch, the surface residual stress after cold-bending increased 8 ksi along with an increase in the 10 minute residual stress of 3.5 ksi. Comparing Figure 4-16 to Figure 4-17 shows that residual stresses of the 1100°F uniform temperature and the 1200°F surface temperature increased slightly. One reason for this small increase in the surface residual stresses is that the stress-strain curves at both 1100°F and 1200°F are close to bilinear, allowing an increase in the strain while the stress in the material remains relatively constant. In Figure 4-18 the residual stresses for a 2-inch thick plate are shown with the same pattern of an increase in residual stress as the plate is bent at the various temperatures. The plate temperatures after 5 and 10 minutes of cooling were approximately 360°F and 240°F for the 1-inch thick plate, 480°F and 300°F for the 1.5-inch plate, and 560°F and 380°F for the 2.0-inch plate.

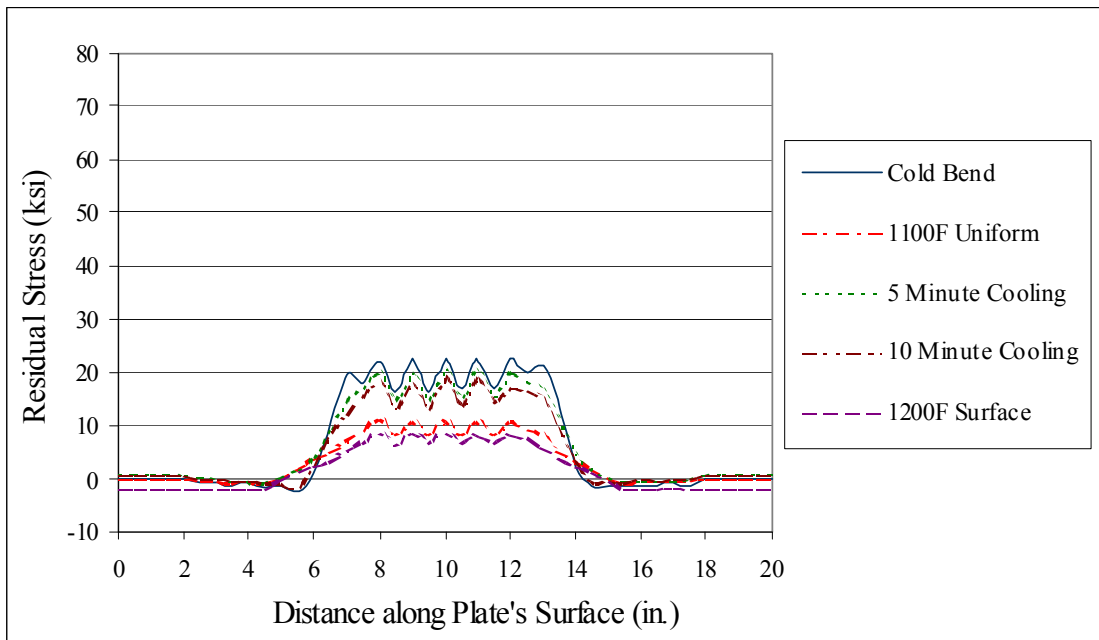


Figure 4-16. Surface Residual Stress 1-Inch Plate - 50 ksi.

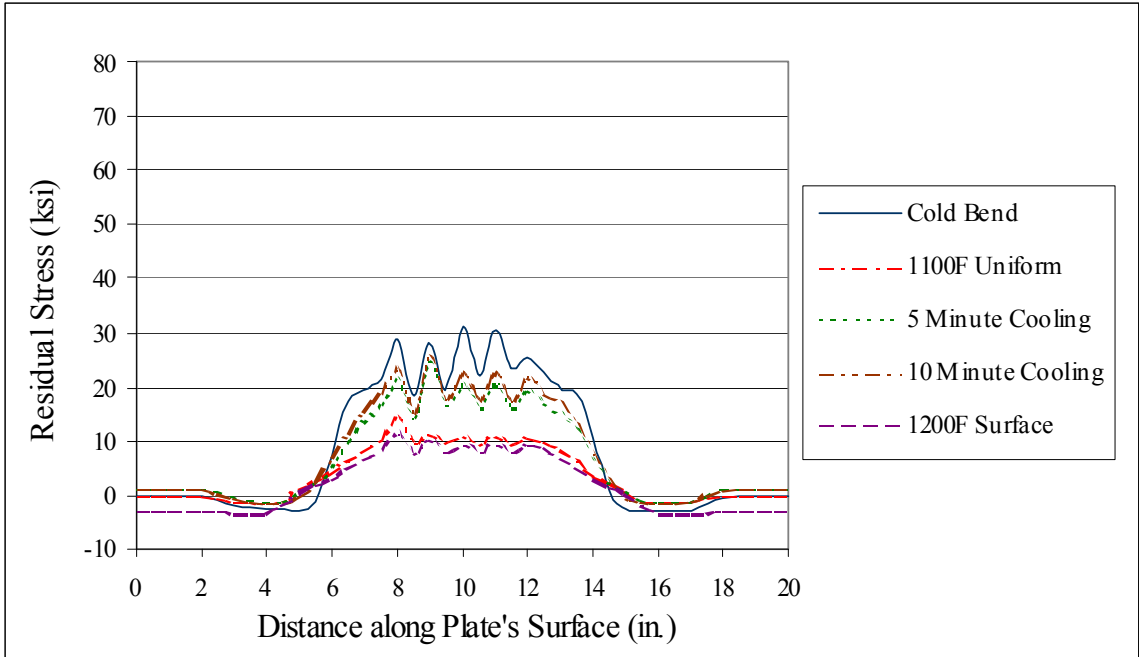


Figure 4-17. Surface Residual Stress 1.5-Inch Plate - 50 ksi.

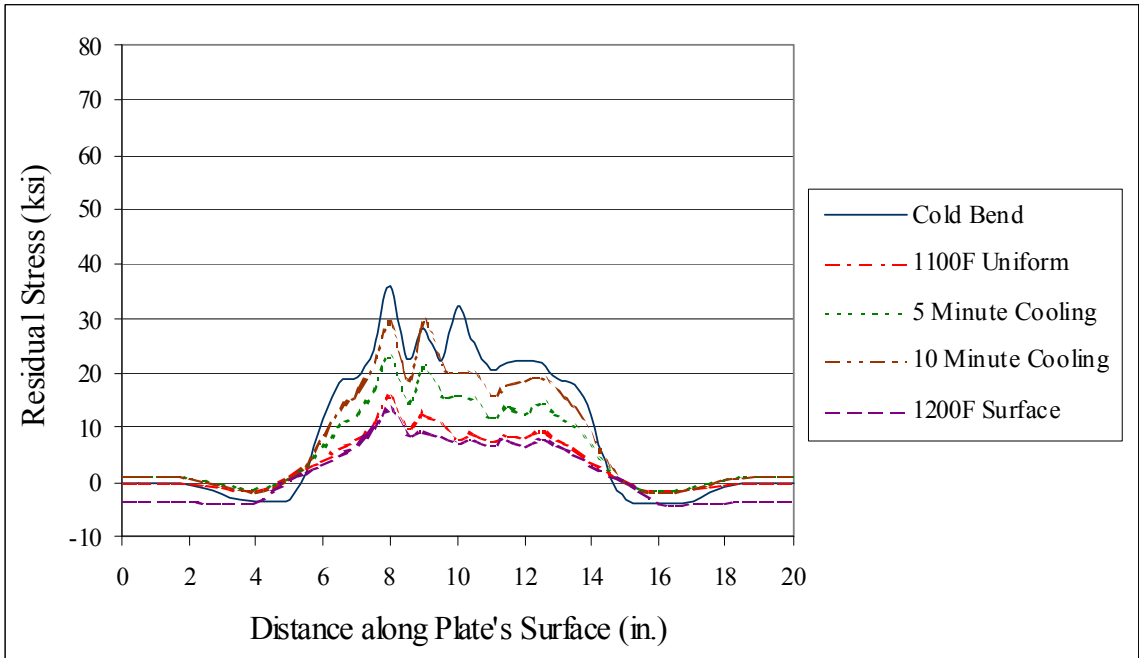


Figure 4-18. Surface Residual Stress 2-Inch Plate - 50 ksi.

4.6.7 Strain along the Plate's Surface

The amount of surface strain present in the plate after bending is related to the severity of the initial bend, which is directly related to the degree of springback occurring in the plate after the load is released. Another factor is the plate's thickness. One equation given by the [ASME \(2004\)](#) Boiler and Pressure Vessel Code (section UCS-79) relates the thickness of the plate to the extreme fibers' elongation (Eq. [2-1]). Others, such as [Weng and White \(1990a\)](#), discuss different equations that can be used to determine the magnitude of surface strain that can occur due to a certain bend radius (Eq. [4-1]). The use of these two equations provides a check of the finite element model to determine if the results between these equations coincide with the results given by ANSYS 8.0. In

[Table 4-1](#), the extreme fiber strains determined by the finite element program are compared to the equations in the Boiler and Pressure Vessel Code and the equation cited by [Weng and White \(1990a\)](#). The average strain along the plate's surface affected by the bending was very similar to the predicted values, with the greatest difference being 1.4 percent. Since the difference in the predicted values given by the two equations and the values obtained from ANSYS were so similar, it was determined that the finite element model could be considered correct within reasonable error.

$$\% \text{ extreme fiber elongation} = \frac{50t}{R_f} \left(1 - \frac{R_f}{R_o} \right) \quad (4-1)$$

$$\epsilon_{\max} = \frac{1}{1.8 \frac{R}{t} + 1} \quad (4-2)$$

Table 4-1. Comparison of Surface Strains.

Plate Thickness (in.)	ASME Code (%)	Weng and White (%)	ANSYS 8.0 (Cold Bend) (%)	Difference from ASME Code (%)	Difference from Weng and White (%)
1	8.3	8.5	7.1	1.2	1.4
1.5	12.5	12.2	11.5	1.0	0.7
2	16.7	15.6	15.6	1.1	0.0

The surface strains in [Figure 4-19](#) for the 1-inch thick plate only extend 2 inches beyond the first and last loading of the plate, with peak strains occurring at each of the five loading points. If the fabricator is slightly off of the 6-inch radius bend, the magnitude of residual strains that the plate experiences can be greatly influenced by the fact that loading the plate takes the steel into the plastic region of the stress-strain curve. Therefore, a small change in the material's stress can greatly affect the amount of strain that will occur. For this reason, all plates were modeled to be within 0.1 inch of the correct radius at all points. The results for the 1.5-inch plate are shown in [Figure 4-20](#) and the results of the 2-inch plate bent to a 6-inch radius are shown in [Figure 4-21](#). Each of these graphs follows the same behavior of the 1-inch plate thickness with only the strain changing 4 to 8 percent in magnitude between the plate thicknesses.

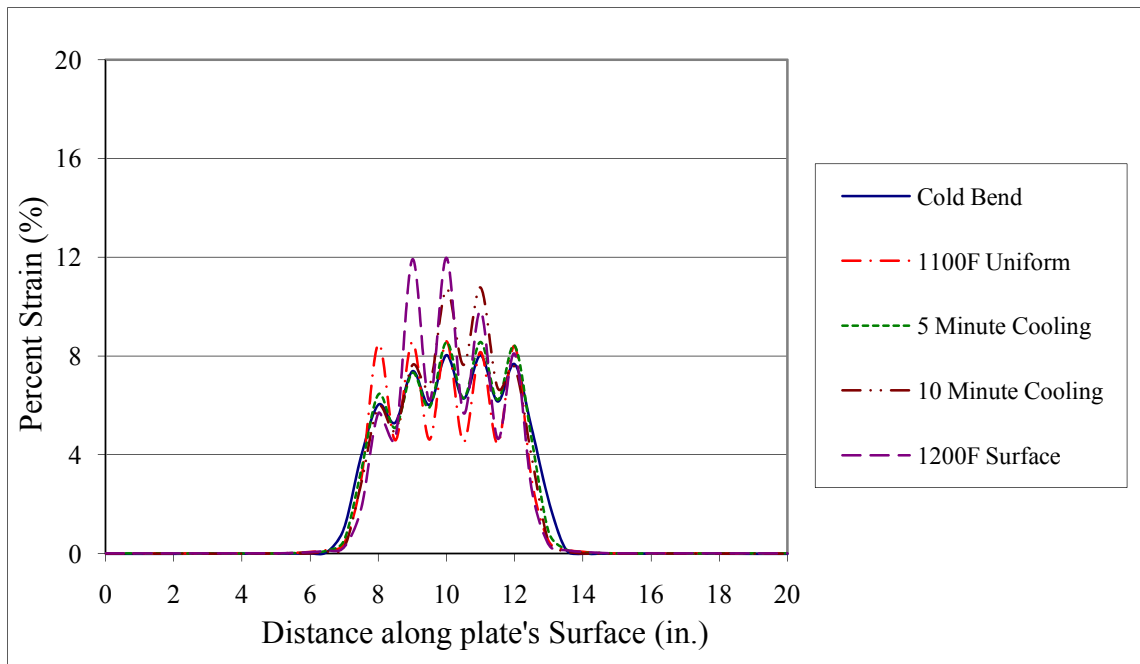


Figure 4-19. Surface Strain 1-Inch Plate - 50 ksi.

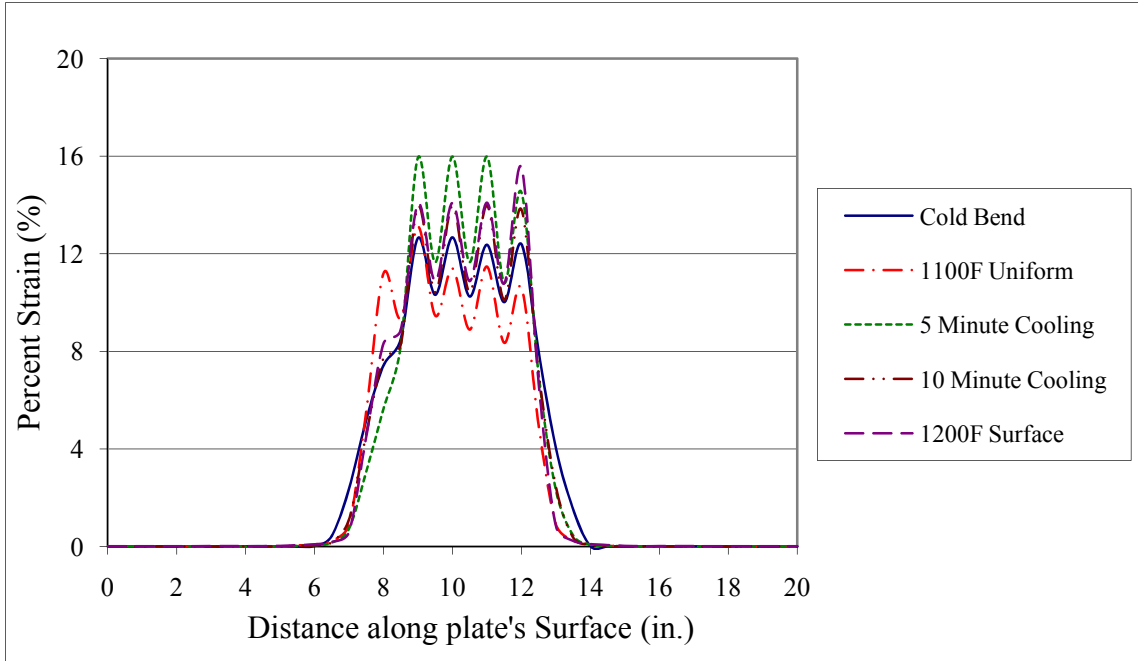


Figure 4-20. Surface Strain 1.5-Inch Plate - 50 ksi.

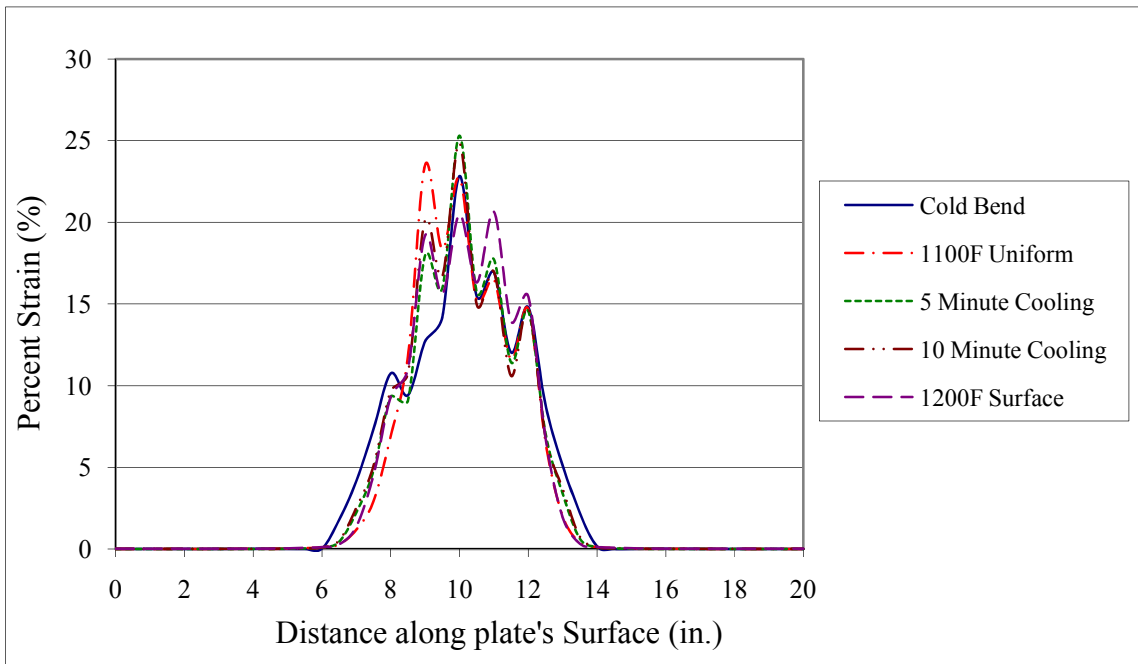


Figure 4-21. Surface Strain 2-Inch Plate - 50 ksi.

The above figures show to what degree loading affects strains along the steel's surface. However, it was determined that strain results would be shown at only one location along the plate's surface in order to get a clearer understanding of how the temperature gradients affect the strains before and after the load passes a location. The location that was selected for observation was the location directly below the load that was applied during load step three. This location was chosen because of the fact that five point loads were used to obtain the correct bend so there was an equal number of hits before and after the point of observation. In [Figure 4-22](#), very little strain was observed during the first two loadings but strain level increased significantly when the load was applied directly at the observed location. As the load was removed strain decreased slightly for all temperatures studied due to the elastic springback as the plate was unloaded. When the next loading occurred 1 inch from the previous location, strain increased but did not reach the magnitude seen when the load was applied directly at the observed location. Observing the strains in the 1.5-inch plate ([Figure 4-23](#)), strains increased as a result of the temperature gradient produced by the plate cooling for 5 and 10 minutes with the cold-bend and 1100°F uniform temperature having approximately the same strain. In [Figure 4-23](#), this same observation can be made with the exception of the 1-inch plate that was allowed to cool for 5 minutes. One reason that the 1-inch plate did not increase in strain after 5 minutes of air-cooling could be that after 5 minutes of cooling only a small temperature gradient was present. When the plate thickness increased to 1.5 and 2 inches, the temperature gradient was more substantial and had a greater influence on the amount of residual strains that occurred. In [Figure 4-24](#), the resulting strains for the 2-inch plate follow the same pattern as those of the 1.5-inch plate, with the only difference being the 1200°F torch heating. The strains resulting from the bending of a 2-inch plate at 1200°F were less than those of the other temperatures studied. The amount of strain occurring at 1200°F is more susceptible to the amount of deflection occurring at the bend location than would otherwise be encountered at lower temperatures because the stress-strain curve at 1200°F closely resembles a bilinear curve.

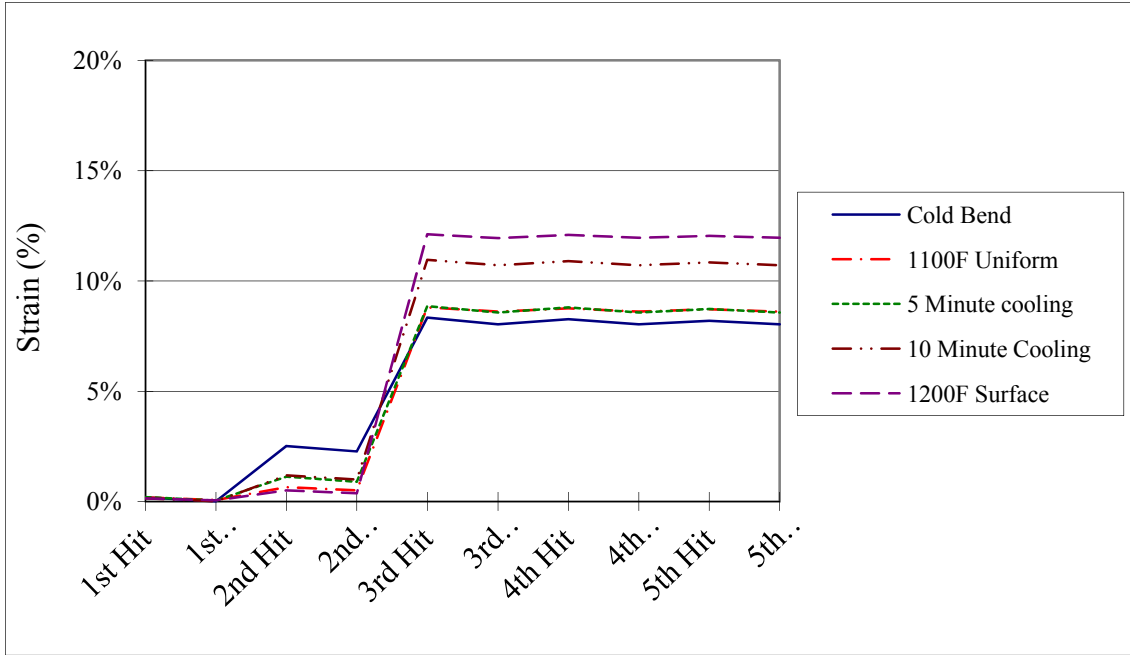


Figure 4-22. Surface Strain at a Point 1-Inch Plate - 50 ksi.

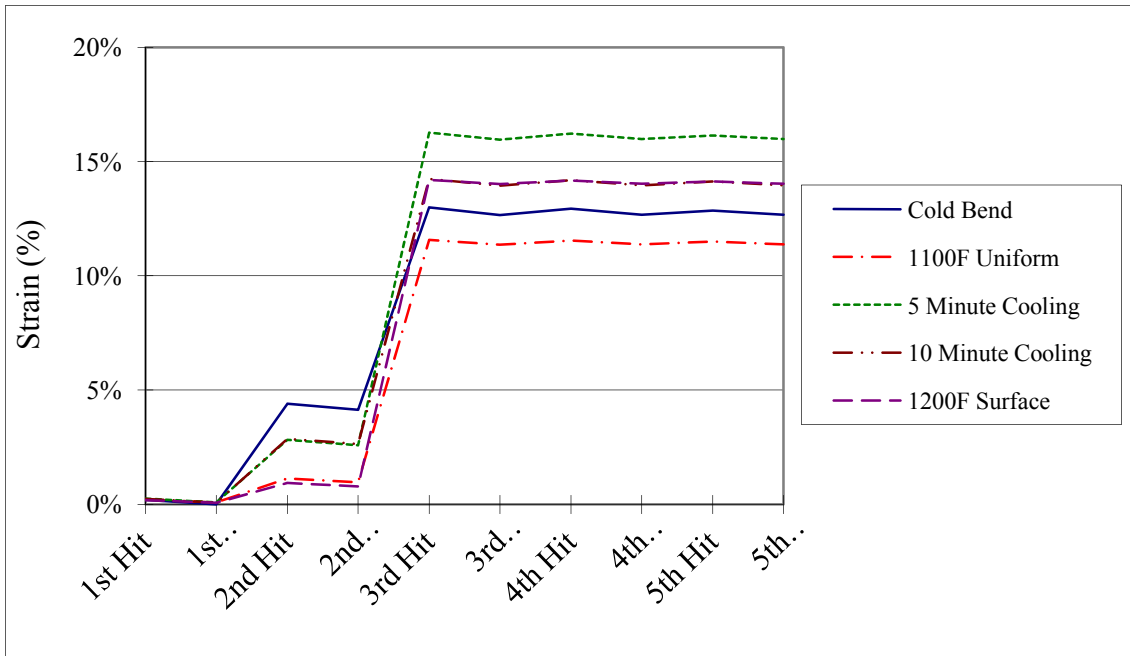


Figure 4-23. Surface Strain at a Point 1.5-Inch Plate - 50 ksi.

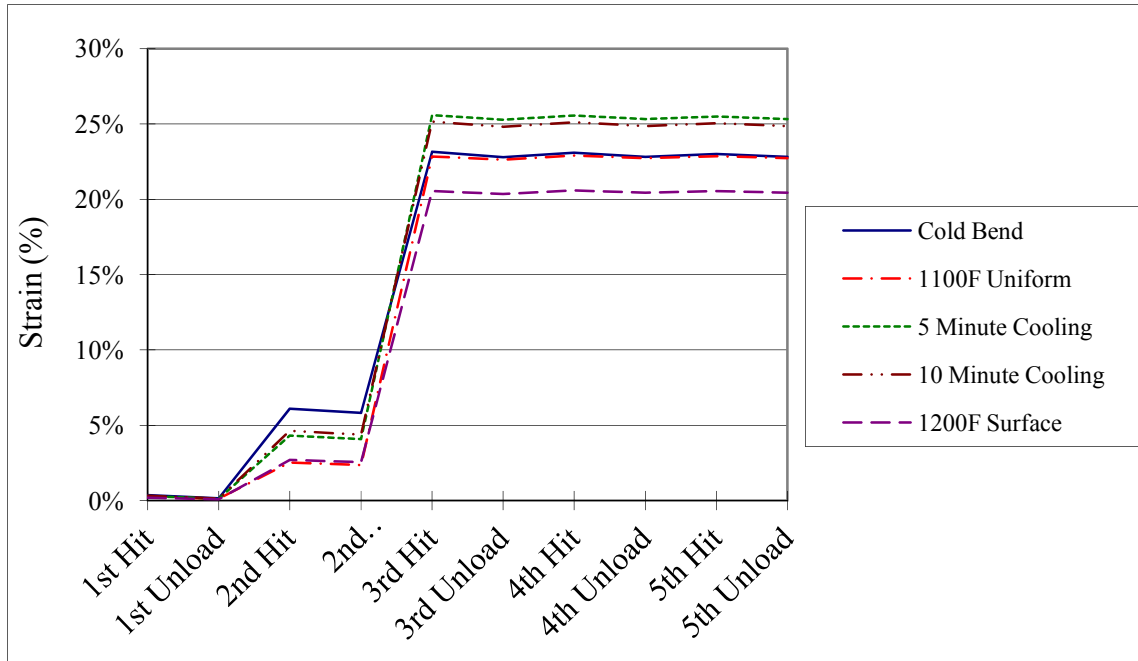


Figure 4-24. Surface Strain at a Point 2-Inch Plate - 50 ksi.

The [ASME \(2004\)](#) Boiler and Pressure Vessel Code (section UCS 79) sets a 5 percent limit on the amount of strain increase from the as-rolled condition before stress-relieving heat treatment must be applied after the fabrication process is complete. Another restriction on the fabrication of boiler and pressure vessels is that if the material is formed in the temperature range of 250°F to 900°F the material has to undergo heat treatment after forming. This rule for temperature during forming was put into place to reduce the effects of the temperature gradient and the formation of residual stresses. The temperature limits are also intended to keep the steel out of the blue brittleness range during fabrication. After 5 and 10 minutes of air-cooling, all of the plates studied were in this temperature range, requiring heat treatment, except for the 2-inch thick plate that was air-cooled for 5 minutes. To further substantiate the need for heat treatment after bending, all plates that were studied exceeded the 5 percent limit on strain set by the [ASME \(2004\)](#) Boiler and Pressure Vessel Code. Some researchers have stated that the 5 percent limit is too conservative for today's clean steel and have proposed a higher limit of 7 percent ([Bala and Malik 1983](#), [Blondeau et al. 1984](#)), but even at this elevated limit, all plates studied would still require heat treatment even without consideration of the bending temperature. Because of this 5 percent strain limit, researchers decided to investigate the amount of strain needed at the time of bending to achieve the final 5 percent strain and to determine if the radius could be obtained at

this strain limit. In [Table 4-2](#), the initial strains needed to obtain the 5 percent final strain for the various plate thicknesses and grades of steel vary from around 5.3 percent to as high as 5.5 percent. With the ASME Boiler and Pressure Vessel Code strain limits, the radius of bend that can occur before heat treatment is required is 10 inches for a 1-inch thick plate, over half again the radius that is desired by some in the bridge fabrication industry. Therefore, following the [ASME \(2004\)](#) code requirements, heat-treatment would always have to be performed after completion of the bending process. The same observations can be made for steel having a yield strength of 70 ksi (see [Christian 2005](#)).

Table 4-2. Five Percent Strain.

Thickness (in.)	Yield Stress (ksi)	Load at Midspan (kips)	Initial Strain (%)	Final Strain (%)
1	50	40.8	5.3	5.0
1.5	50	86.4	5.4	5.1
2	50	150	5.4	5.1
Thickness (in.)	Yield Stress (ksi)	Load at Midspan (kips)	Initial Strain (%)	Final Strain (%)
1	70	55.9	5.4	5.0
1.5	70	91.5	5.4	5.0
2	70	200	5.5	5.0

4.6.8 Through-Thickness Stresses

The through-thickness stress distributions remained relatively constant for the different plate sizes and the various steel grades studied. Because of this, only the 1-inch plate thickness for the 50 ksi steel will be discussed, with the remaining results for the other plate thicknesses found in ([Christian 2005](#)). In [Figure 4-25](#) to [Figure 4-28](#), the graphs refer to various hits. Each of these hits was observed at a single location to determine what effect multiple bend points in the fabrication of bent flange plates would have. The location through the plate's thickness that was chosen as the point of reference was the location directly below the load application for the third bend point. The first hit shown in the figures occurs at a point 2 inches from the point of observation, while the next hit progresses 1 inch toward the point, and after the third hit the next two hits continue past the point of observation at 1-inch intervals.

When looking at the results graphed in [Figure 4-25](#) through [Figure 4-28](#), the highest stresses occurred during cold-bending while the lowest occurred when the plate's surface was

heated to 1200°F. This result can be explained by the simple fact that the magnitude of the stress-strain curve for steel is much higher at low temperatures than at high temperatures. The graphs also indicate that the highest stresses through the plate's thickness occur when the load is applied directly above the location under consideration, with the stress decreasing after the load passes. The temperature at bending with 10 minutes of cooling was approximately 250°F.

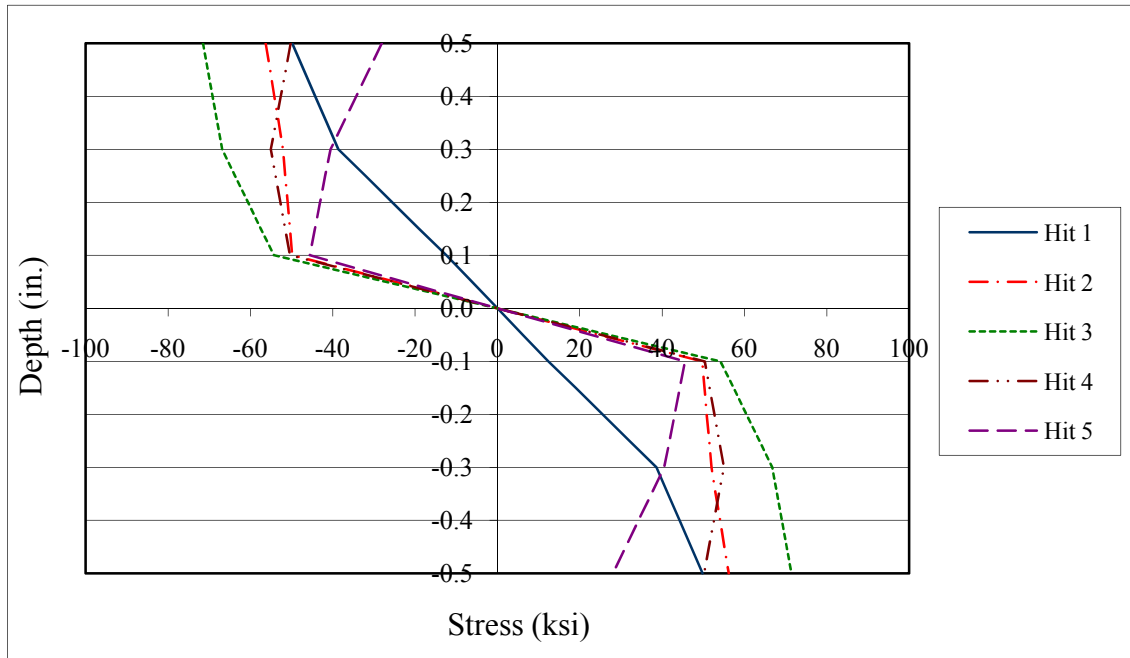


Figure 4-25. Through-Thickness Stress Cold Bend - 50 ksi.

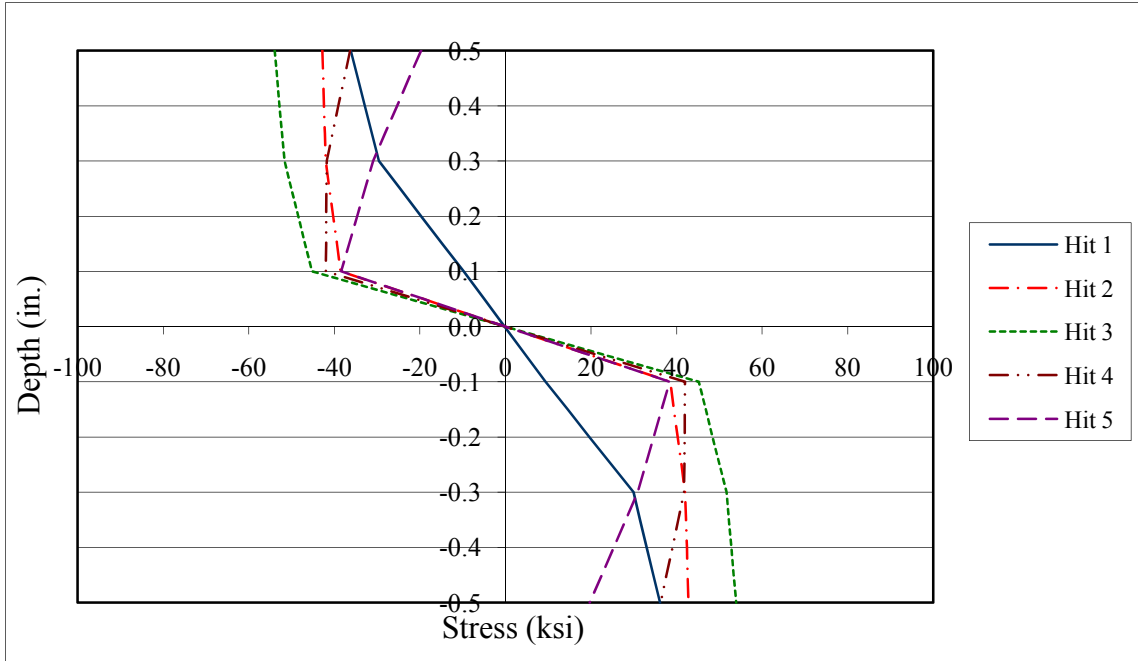


Figure 4-26. Through-Thickness Stress 10 Minute Cooling - 50 ksi.

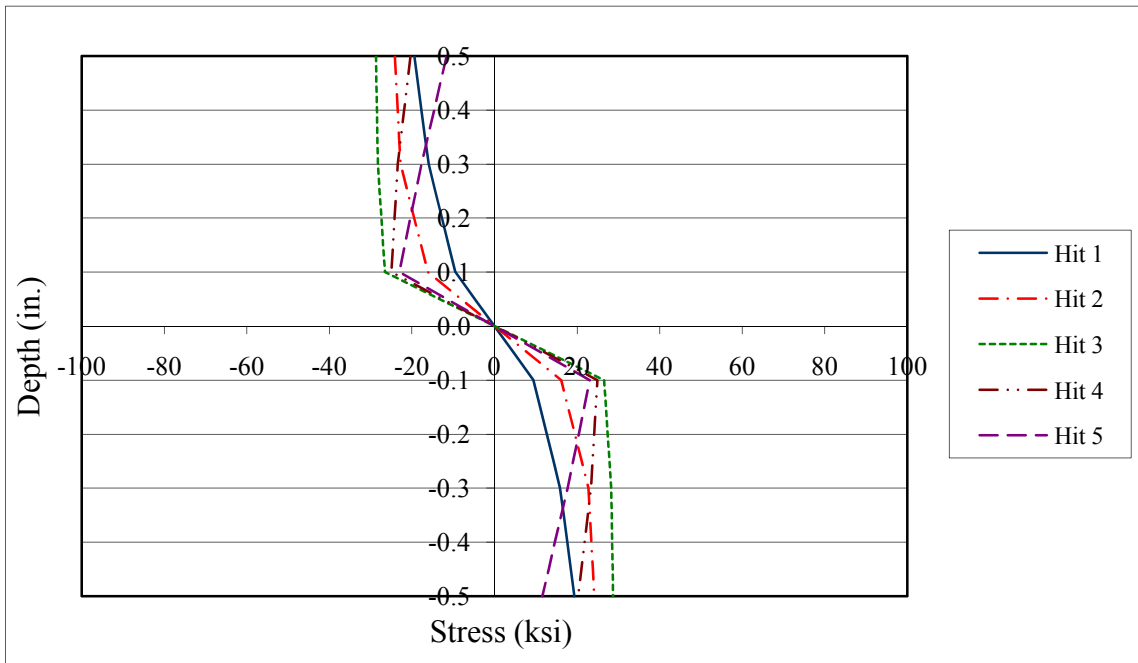


Figure 4-27. Through-Thickness Stress 1100°F Uniform Temperature - 50 ksi.

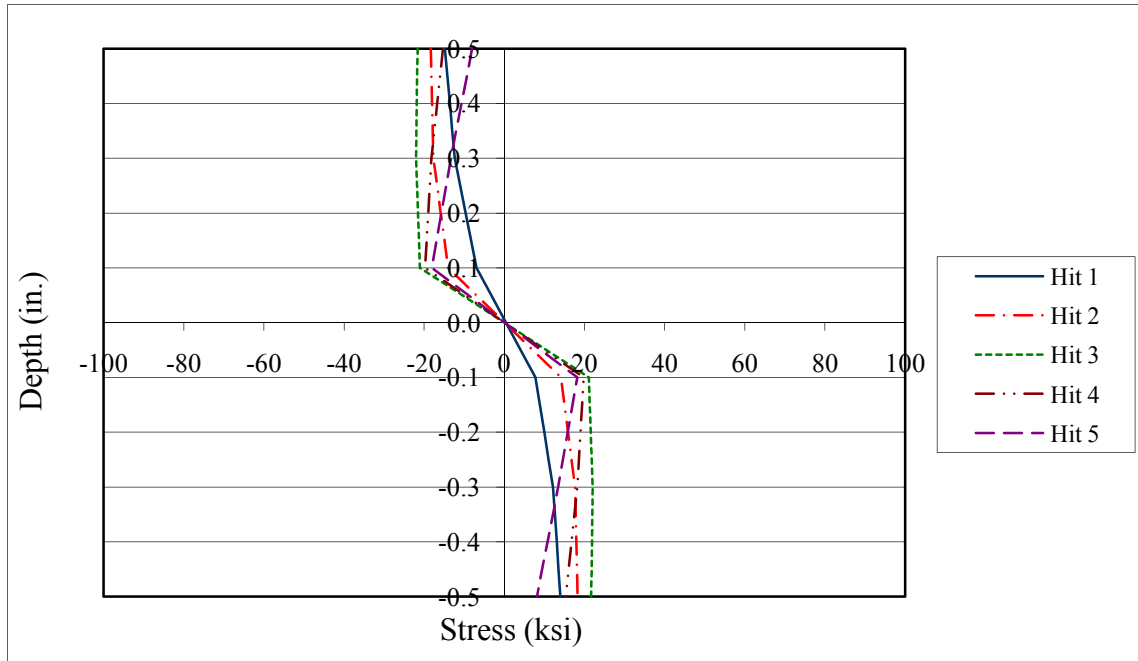


Figure 4-28. Through-Thickness Stress 1200°F Surface Temperature - 50 ksi.

As the load approached the measurement point, the fibers yielded within 0.1 inch of the neutral axis. One of the drawbacks of using the finite element mesh of 0.2-inch squares is that the material can only yield to a node closest to the neutral axis, which for a Quad 8 Node 82 at that mesh size is 0.1 inch. This restriction is brought about by one of the principles in mechanics of materials that some portion around the neutral axis of the plate will always behave elastically (Boresi and Schmidt 2003). For the plate that was air-cooled for 10 minutes after obtaining an 1100°F uniform temperature and then underwent the bending process the stresses are shown (Figure 4-26) to resemble those of cold-bending. Comparing the stresses between cold-bending and air-cooling for 10 minutes, the difference was only 10.6 to 17.5 ksi 0.15 inches from the neutral axis and extreme fiber, respectively; these differences in stress will later be shown to result in a very small reduction in the residual stress through the plate's thickness. When the plate was bent at both a uniform temperature of 1100°F and with a 1200°F surface temperature, the temperature in the plate caused a large reduction in the plate's through-thickness stresses. The behavior of the plate bent at 1100°F, shown in Figure 4-27, continues the pattern discussed but with the increase in the plate's temperature the stress curve at hit three holds a constant stress through the plate's thickness. The reason for this is the stress-strain curve (Figure 4-13), which resembles a bilinear curve, and the benefit to this is that as the load increases, the strain in the

material increases while the stress remains constant. Therefore, the residual stresses are constant after a certain level of stress is reached. For a plate that was bent after torch heating (Figure 4-28) the stresses were further reduced compared to what the uniformly heated plate experienced. After the load passes, a certain location of the stress in the plate will no longer be affected by the load being applied. This was seen after the load had progressed 2 inches past the point of observation, shown as hit five in Figure 4-28.

4.6.9 Through-Thickness Residual Stresses

The magnitude of stress through the plate's thickness indicates whether residual stresses will occur in the plate after the plate is unloaded. If the stress passes the yield point of the material and moves into the plastic region of the stress-strain curve, a residual stress will remain after unloading. The amount of stress remaining is directly related to the magnitude of strain that developed during the loading process. When considering the residual stress distribution through a plate's thickness, one area of consideration was the amount of tensile residual stress on the inside surface of the plate bend, for it could cause cracking and stress corrosion (Weng and White 1990a).

After each loading phase, the plate was allowed to unload to simulate using a brake press to fabricate the bent flange plate. In Figure 4-29 thru Figure 4-32, the through-thickness residual stresses were observed at the same location that was used in the previous section, under the location where the third loading occurred. Following this procedure, it was observed that in all of the plate thicknesses studied, the residual stresses are at their highest levels at the applied load location. And, as the load progressed past the previously loaded location the residual stresses remain relatively constant.

When comparing the residual stresses caused by bending a plate at room temperature (Figure 4-29) to those of the other temperatures studied, the plate undergoes the largest magnitude of residual stress. The tensile residual stress on the inside surface of the bent plate was 23 ksi. This extreme fiber residual stress is approximately one-half of the yield strength of the material studied. This residual stress indicates that a large amount of plastic deformation occurred in the plate at the time of bending. As the residual stresses approach the neutral axis, the stresses change from tensile to compression with the maximum residual stress occurring 0.1 inch from the neutral axis. The maximum residual stress at that location was 35 ksi. When

looking at the plate after cooling from 1100°F uniform temperature and bending (Figure 4-30), the residual stresses were only slightly different than those resulting from cold-bending. The tensile residual stress on the plate's inside surface was 18.7 ksi after the bending process was complete. The residual stress occurring near the plate's neutral axis also decreases slightly, to 30 ksi. There was only a difference of around 5 ksi from the plate that was bent at room temperature to the plate that was bent after it was heated to 1100°F and allowed to air cool for 10 minutes. The plate that was allowed to air cool for 5 minutes from 1100°F uniform temperature and then underwent the bending process also had the same relatively small decrease in the residual through-thickness stress as the plate that cooled for 10 minutes.

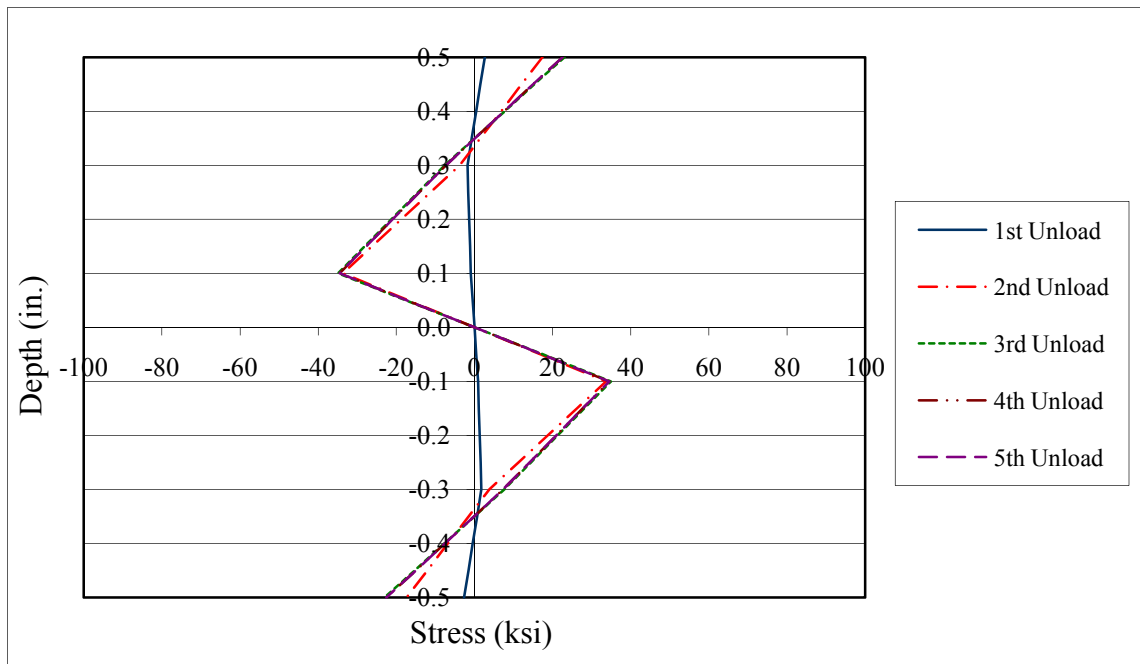


Figure 4-29. Through-Thickness Residual Stress Cold Bend - 50 ksi.

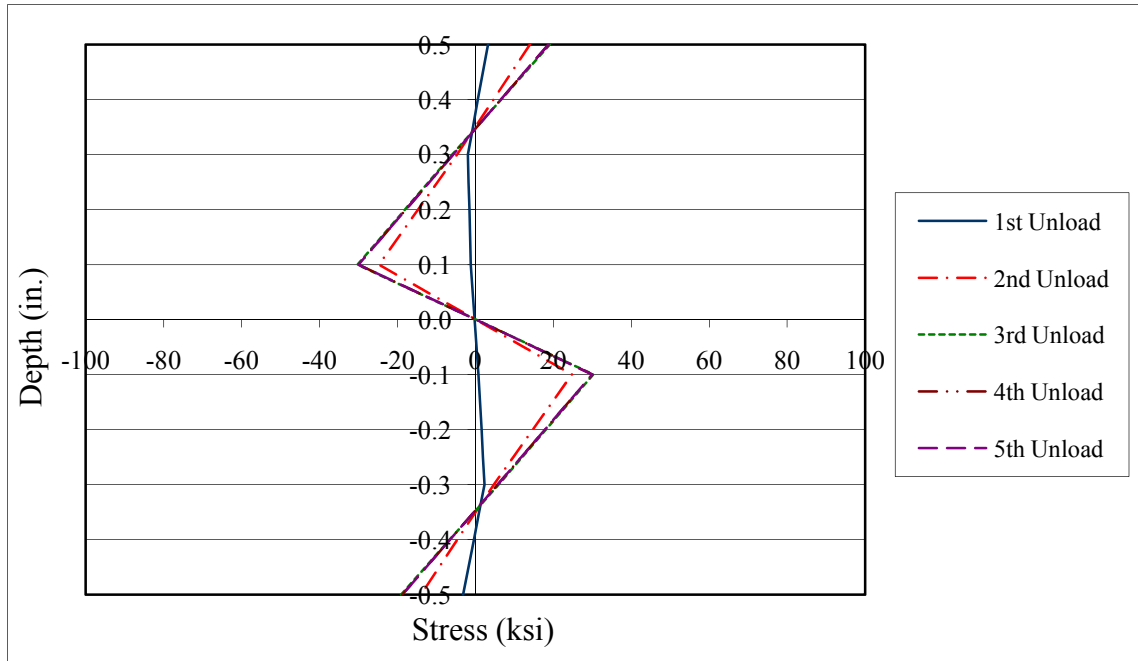


Figure 4-30. Through-Thickness Residual Stress 10 Minute Cooling - 50 ksi.

When the plate was heated to a uniform temperature of 1100°F (Figure 4-31) and immediately bent so that no thermal convection occurred, there was a significant decrease in the residual stress through the plate’s thickness compared to both the plate that was bent at room temperature and the plates that air-cooled for 5 and 10 minutes. This decrease in residual stress was a result of the decrease in the steel’s stress-strain curve, for there is a significant decrease in the amount of stress that the plate can undergo during the bending process. This decrease results in a decrease in the residual stress that develops upon unloading. The tensile residual stress that developed when the plate was heated to 1100°F at the extreme fibers was 11 ksi, which was only about one-half of the residual stress occurring after bending the plate at room temperature. The residual stress near the neutral axis was 18 ksi, also around a 50 percent decrease. When bending the plate after a torch was used to heat the plate’s surface to a temperature of 1200°F, the residual stress decreased even more than when the plate was bent at a uniform temperature of 1100°F. The tensile residual stress at the plate’s extreme fiber was 8.5 ksi (Figure 4-32), and the residual stress found next to the plate’s neutral axis was 14.5 ksi.

Residual stresses were significantly lower when the plate was bent at either 1100°F uniform temperature or after the plate was heated using a torch to a surface temperature of 1200°F than the residual stresses after cold-bending. When the plate was heated to 1100°F and

cooled for 10 minutes before bending, there was a significant increase in the amount of residual stress that occurred as a result of the bending process. This increase in residual stress was a result of the increase in the steel's stress-strain curve.

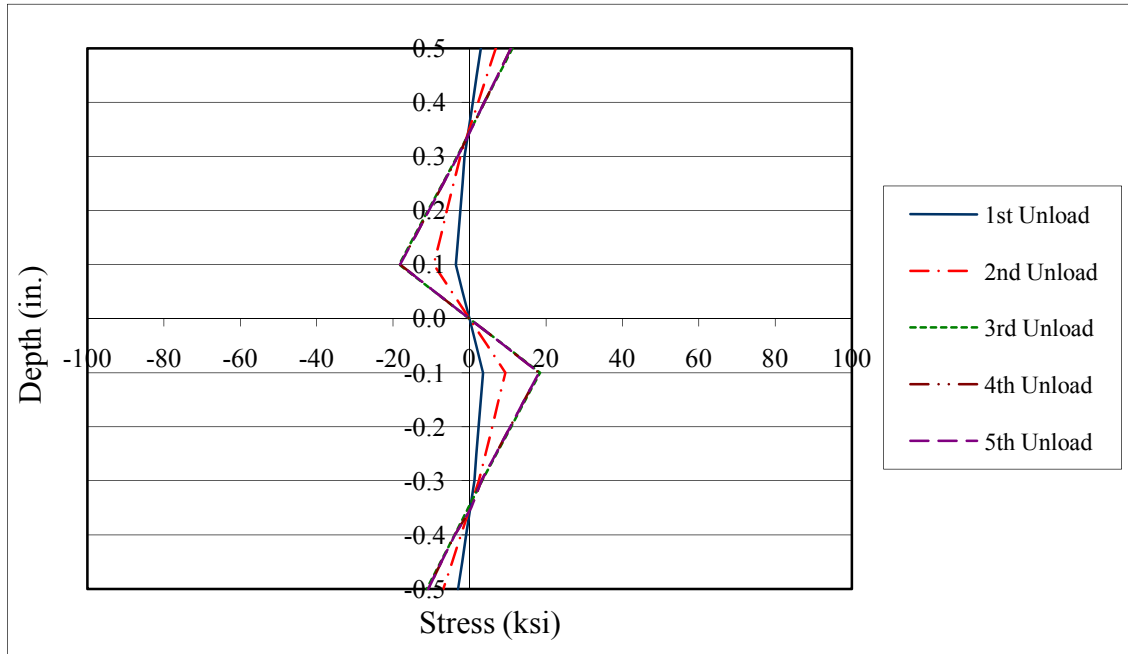


Figure 4-31. Through-Thickness Residual Stress 1100°F Uniform - 50 ksi.

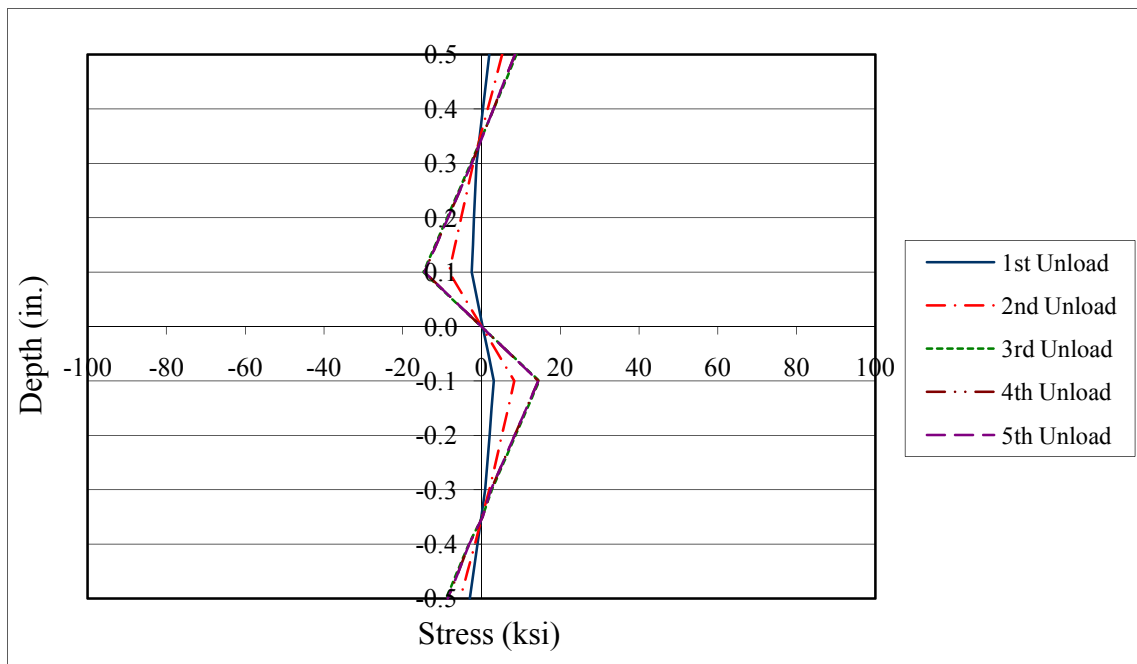


Figure 4-32. Through-Thickness Residual Stress 1200°F Surface Temperature - 50 ksi.

4.7 SUMMARY AND CONCLUSIONS

Research reported herein was conducted to obtain a better understanding of how heating to elevated temperatures affects the residual stress and strain distributions that result from the bending of the flange plate. As a result of this study, several conclusions can be drawn about the different methods of heating and whether the resulting temperature gradients could be a significant factor in causing flange cracking. The conclusions drawn from this in-depth study are as follows.

4.7.1 Thermal Conclusions

- The temperature gradient through the plate's thickness increases as the plate's thickness increases.
- As the thickness of the plate increases so does the time it takes the plate to cool to its original temperature.
- The thermal expansion resulting from torch heating causes compression stresses to form on the plate's extreme fibers. When the plate is then air-cooled from a uniform temperature tensile stresses form on the plate's surface.

4.7.2 Structural Conclusions

- Observing the plate's strain at a point along the plate's surface during the bending process, plates that had temperature gradients present during bending had higher strains than plates that were bent at a uniform temperature.
- In the region of 10 percent of steel's uniaxial stress-strain curve necking can occur. This necking during a uniaxial test results in cracking when the same strain level is observed during the plate bending process. As a result of this both the 1.5- and 2-inch plates exceed this strain level and can, therefore, develop cracks as a result of excessive strains.
- The 6-inch radius bend, for all the plate thicknesses tested, exceeded the strain limits of the [ASME \(2004\)](#) Boiler and Pressure Vessel Code.
- After the plate was heated to a uniform temperature of 1100°F and air-cooled for 5 minutes, the residual stresses after bending the plate to a 6-inch radius were significantly higher than what would have been experienced if the plate were bent

at a uniform temperature of 1100°F. This same result was observed when the plate was air-cooled for 10 minutes before bending. The stresses formed during air-cooling are of the same magnitude as the stresses formed during cold-bending.

- When the plate was bent after torch heating the residual stresses were lower than any other temperature tested. The next lowest surface residual stress occurred when the plate was bent at a uniform temperature of 1100°F.
- The region affected by the bending process was two times the plate's thickness.
- The addition of heat during the fabrication process is beneficial as long as no temperature gradients are present at the time of bending. Temperature gradients increase the likelihood that cracking of the flange plate can occur.

CHAPTER 5: FATIGUE BEHAVIOR OF NON-LOADED BOLTED CONNECTIONS

5.1 GENERAL

The fatigue strength of bolted connections is classified by AASHTO as Category B. In order to achieve this fatigue strength, the bolts must be properly pre-tensioned. The improved fatigue strength is achieved by the change in load transfer through the connection from bolt bearing to friction between the faying surfaces. This change in load transfer reduces or eliminates the stress concentration around the bolt holes, thereby increasing the fatigue strength of the detail.

Non-loaded bolted connections occur when secondary members, such as lateral bracing, are attached on primary members or components. While the connection still transfers the secondary forces through the connection in much the same way, the primary member carries significant load unrelated to the secondary members. These forces in the components of primary members pass through relatively unaffected by the bolted attachment and result in stress concentrations around the bolt holes. The bolts must be pre-tensioned in order to shield the bolt holes from fatigue damage. The compressive stress around the bolt holes is greatest at the ends of the hole and can diminish toward the mid-thickness of the plate. A significant reduction of shielding may occur in thicker plates.

5.2 TEST PROGRAM

A total of 32 plate specimens were fatigue-tested. The specimens were 6 inches wide by 60 inches long. Plate thicknesses for the specimens ranged from 0.5 inches to 2.0 inches at 0.25-inch increments to 1.5 inches. This range provided six different plate thicknesses, covering typical flange plate thicknesses used in highway girder construction. While thicker plates are used, it was hypothesized that the reduced shielding effect from the bolt clamping would be noticeable with thicknesses 2.0 inches or less and specimens of greater thickness would yield similar results to those of the 2.0-inch plate thickness.

Plate material was received from a single supplier. Mill certifications were obtained for all plates. Material used for a given plate thickness was manufactured from the same heat of steel.

Each specimen had a set of four bolt holes spaced at 3 inches along a longitudinal gage line. The gauge line was located in the middle of the plate width. All hole diameters were 15/16 inch. The holes were either punched or drilled. Twenty six of the specimens were tested with bolted gusset plates, while the remaining specimens were tested with open holes. The gusset plates were 3/8 inch by 6 inches wide by 12 inches long with punched holes. A single gusset plate was used on a given specimen. A325, 7/8-inch diameter high-strength bolts attached the gusset plate to the specimen. The head of the bolt was installed on the opposite side of the gusset plate. A hardened washer was used under the nut. The bolts were pre-tensioned through the turn-of-the-nut method. Pre-tensioning was first performed on the two inner bolts, followed by the outer two bolts. [Figure 5-1](#) shows a specimen with the attached gusset plate.



Figure 5-1. Specimen with Bolted Gusset Plate.

All specimens were cycled at a frequency of 3 Hz under constant-amplitude loading in a 1500 kip capacity load frame (see [Figure 5-2](#)). The test frame was manufactured to test pipe and other circular specimens, so special grip inserts were fabricated for this study to properly grip flat plate specimens. The nominal stress range (based on the gross area cross section) was 25 ksi. Assuming a net hole diameter of 1 inch for the 7/8-inch diameter bolts, the stress range based on the net cross-sectional area was 30 ksi. Several specimens were measured by strain gauge to verify that the applied load ranges were correct. A minimum load of approximately 10 kips was used for each specimen. Each specimen was cycled to until a fatigue crack developed at a hole or for a maximum of approximately 3 million cycles.

The length of each specimen was 5 feet. This length allowed for a 12-inch grip length at either end of the specimen and a 36-inch gage length. The specimens did not have a reduced cross section in the gauge length in an effort to reduce specimen cost. This led to fatigue failure of several specimens within the gripped cross section. However, these specimens (B-7 and C-4) were repaired by grinding and welding the two sides of the fatigue fracture back together. As a result of these grip region failures, specimens that exceeded 500,000 cycles were periodically re-gripped, decreasing the overall gauge length by 1.0 inch at either end of the specimen. This helped force any crack developing in the grip region to re-initiate at a new location, thereby delaying crack propagation.



Figure 5-2. 1.5 Million Pound Capacity Load Frame with Non-Loaded Bolted Connection Specimen.

5.3 HOLE PUNCHING

The hole punching operation was conducted under controlled conditions using a 500-kip test frame mounted with a punch and die set (see [Figures 5-3](#) and [5-4](#)). The punch diameter was 15/16 inch, while the die had a diameter 1/32 inch larger (31/32 inch). Holes were first located

on the specimens and center-punched. A typical set of load-displacement relationship curves is given in [Figure 5-5](#). As expected, the holes in thicker plates required higher punching loads.



Figure 5-3. View of Hole Punching Operation with Specimen C-1.



Figure 5-4. Close-Up View of Punch and Die for Specimen Hole Punching.

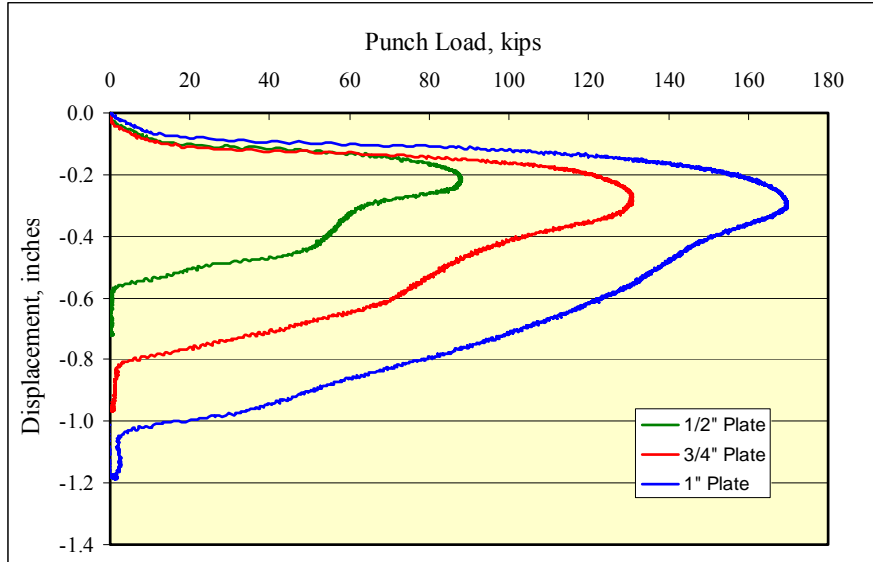


Figure 5-5. Plot of Punch Load versus Displacement for Plate Thicknesses of 0.5, 0.75, and 1.0 Inches.

Figure 5-6 shows typical slugs that resulted from the punching operation for the three plate thicknesses used. A significant characteristic is the layered appearance of the perimeter surface of each slug. Hole punching is primarily a shearing operation. Each layer represents an off-vertical shear plane that formed as the die moved through the thickness of the plate. While the shear plane forms at approximately 45 degrees, it is confined to the vertical plane of the forming hole circumference and must therefore reform. Thicker plates require more shear planes to form than thinner plates during the punching operation.



Figure 5-6. Hole Slugs for Three Plate Thicknesses Resulting from Punching Operation.

5.4 TEST RESULTS

The test matrix and corresponding fatigue test results for each specimen are provided in [Table 5-1](#). A total of 37 million cycles were accumulated on the specimens shown in the test matrix. Note that for plate thicknesses up to 1.0 inch, both punched and drilled holes were used. However, only one specimen each was used for a drilled hole, with or without a gusset plate. For plate thicknesses 1.25 inches or greater, only drilled holes were tested (with and without a gusset plate) due to the limitations on the ability to punch holes in thick plates. Hole punches are typically manufactured for use on a maximum plate thickness of 1.0 inch. To punch holes through plates of greater thickness requires longer punches that are susceptible to stability issues, especially for the smaller diameter holes. Additionally, the force required to punch thicker plates normally exceeds the capacity of standard punching equipment.

For both sets of specimens (with and without a gusset plate) fatigue failure occurred at either of the outer holes. For the specimens with gusset plates, the crack initiated on one side of the hole, perpendicular to the longitudinal axis of the specimen (3 and 9 o'clock position) and maximum concentrated stress field around the hole. [Figure 5-7](#) provides a view of the fracture surface typical for the specimens without a gusset plate. For specimens with gusset plates, the crack initiation location was influenced by the plate thickness. For the thinner plates, the crack initiated off the perpendicular plane, more toward the end of the gusset plate. This crack orientation can be seen in [Figure 5-8](#) for Specimen B-4. With increased plate thickness, crack initiation shifted back to the 3 and 9 o'clock position as shown in [Figure 5-9](#).

[Figures 5-10](#) through [5-11](#) show the test data on typical stress range versus number of cycles to failure (S-N) plots with AASHTO Fatigue Categories B, C, and D. As expected, the use of a bolted gusset plate improved the fatigue strength for each of the base plate thicknesses tested. For the punched hole specimens, the percent change in fatigue life improvement is skewed, however, by the fact that the fatigue strength increases with increasing plate thickness for the specimens without gusset plates. This can be seen in the comparison of data in [Figures 5-10](#) and [5-15](#). Therefore, fatigue life improvement was greatest with the 0.5-inch thick specimens. Additionally, it was the 0.5-inch thick bolted specimens that provided fatigue lives greater than 3 million cycles.

Table 5-1. Test Matrix and Results for Fatigue Behavior of Non-Loaded Bolted Connections.

Specimen Number	Hole Type	Gusset Plate	Cycles to Failure	Comment
0.5-inch Plate Thickness				
A-1	Punched	No	356,108	
A-2	Punched	No	346,620	
A-3	Punched	Yes	>4,747,100	Runout – No Failure
A-4	Punched	Yes	3,079,188	
A-5	Punched	Yes	>3,121,724	Runout – No Failure
A-6	Drilled	No	297,421	
A-7	Drilled	Yes	1,784,822	
0.75-inch Plate Thickness				
B-1	Punched	No	543,476	
B-2	Punched	No	459,865	
B-3	Punched	Yes	1,790,467	
B-4	Punched	Yes	2,341,235	
B-5	Punched	Yes	2,905,333	
B-6	Drilled	No	422,324	
B-7	Drilled	Yes		Grip/Edge Failure
1.0-inch Plate Thickness				
C-1	Punched	No	992,083	
C-2	Punched	No	881,277	
C-3	Punched	Yes	1,098,730	
C-4	Punched	Yes	1,869,055	
C-5	Punched	Yes	1,613,510	
C-6	Drilled	No	220,773	
C-7	Drilled	Yes	1,166,692	
1.25-inch Plate Thickness				
D-1	Drilled	No	386,019	
D-2	Drilled	No	591,320	
D-3	Drilled	Yes	2,357,537	
D-4	Drilled	Yes	963,243	
D-5	Drilled	Yes	1,217,707	
1.5-inch Plate Thickness				
E-1	Drilled	No	447,947	
E-2	Drilled	Yes	834,448	
E-3	Drilled	Yes	641,320	
2.0-inch Plate Thickness				
F-1	Drilled	No	499,605	
F-2	Drilled	Yes	616,880	
F-3	Drilled	Yes	771,105	

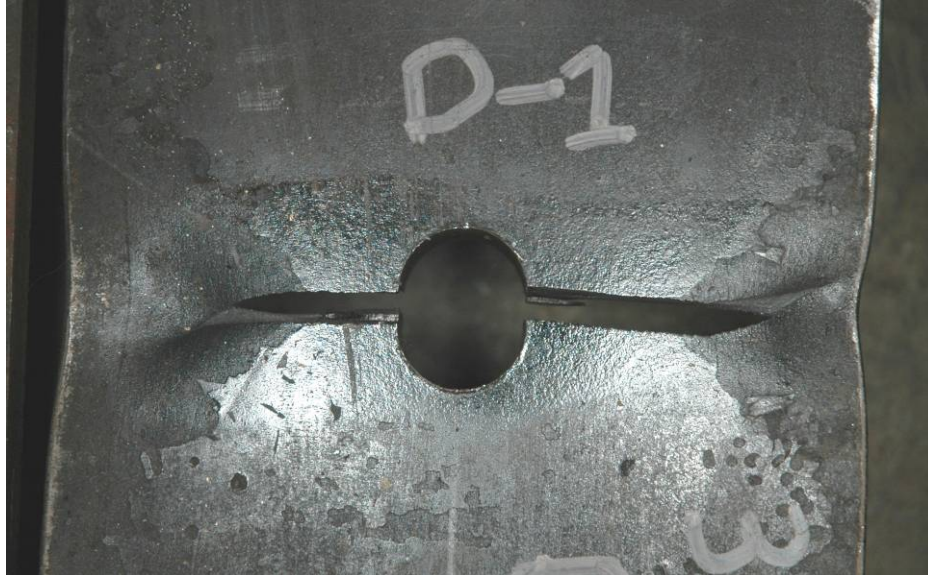


Figure 5-7. Typical Crack Orientation for Specimens with Bolted Gusset Plate (Specimen D-1).



Figure 5-8. Typical Crack Orientation for Thin Plates (<1.0 Inches) with a Gusset Plate (Specimen B-4).



Figure 5-9. Typical Crack Orientation for Thick Plates (≥ 1.0 Inches) with a Gusset Plate (Specimen E-3).

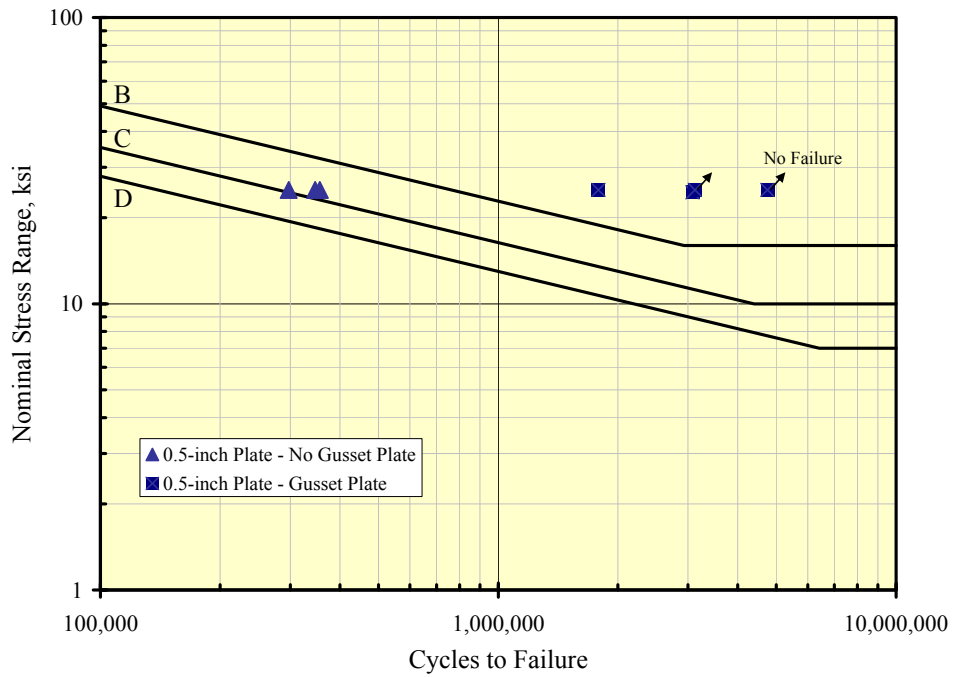


Figure 5-10. Stress Range vs. Number of Cycles to Failure for 0.5-Inch Thick Specimens.

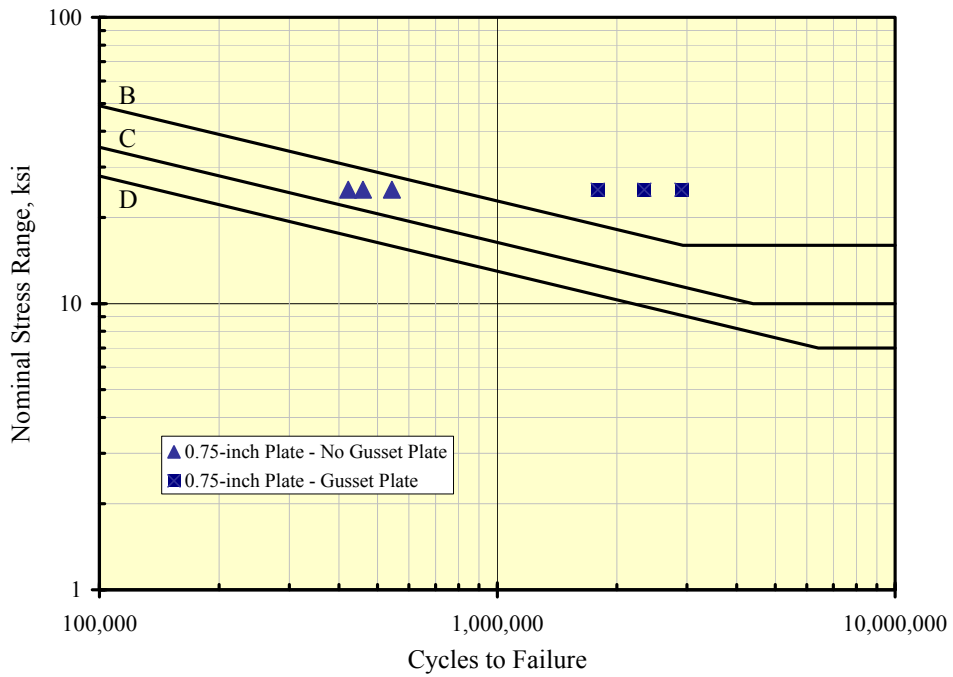


Figure 5-11. Stress Range vs. Number of Cycles to Failure for 0.75-Inch Thick Specimens.

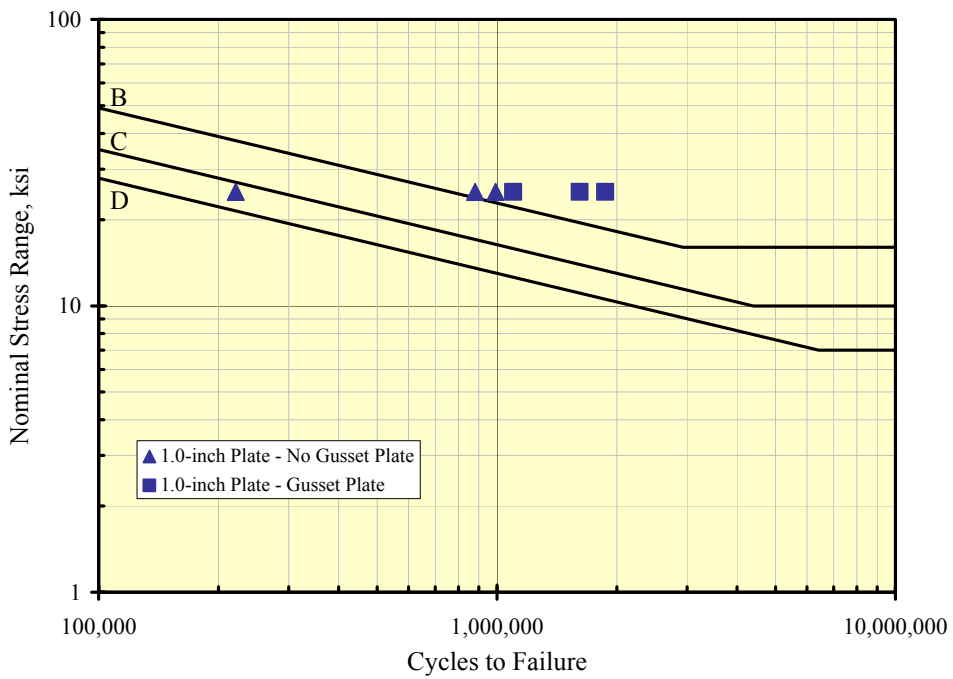


Figure 5-12. Stress Range vs. Number of Cycles to Failure for 1.0-Inch Thick Specimens.

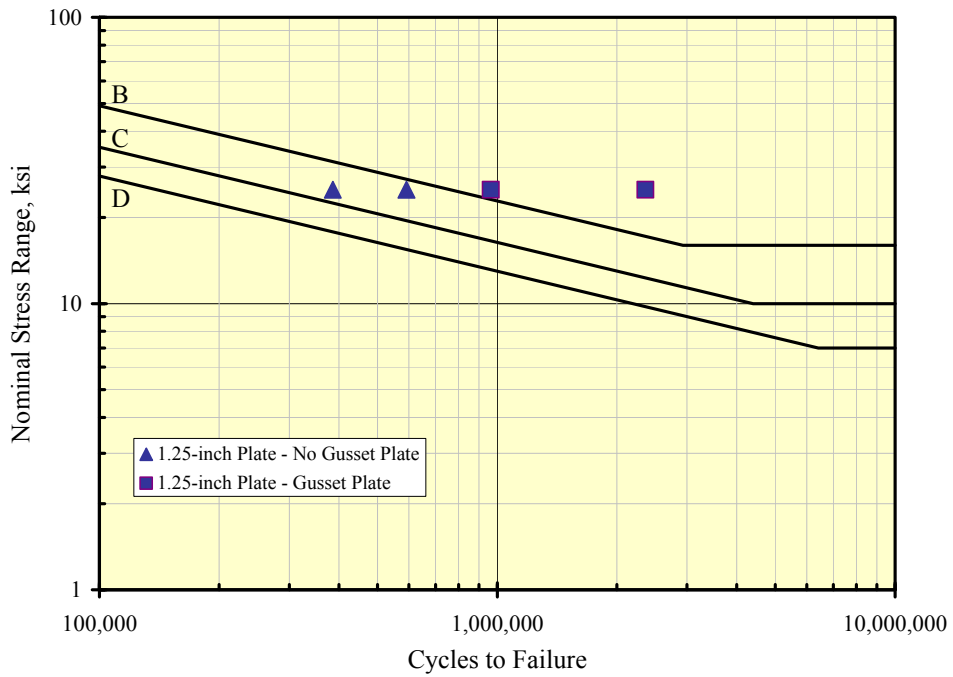


Figure 5-13. Stress Range vs. Number of Cycles to Failure for 1.25-Inch Thick Specimens.

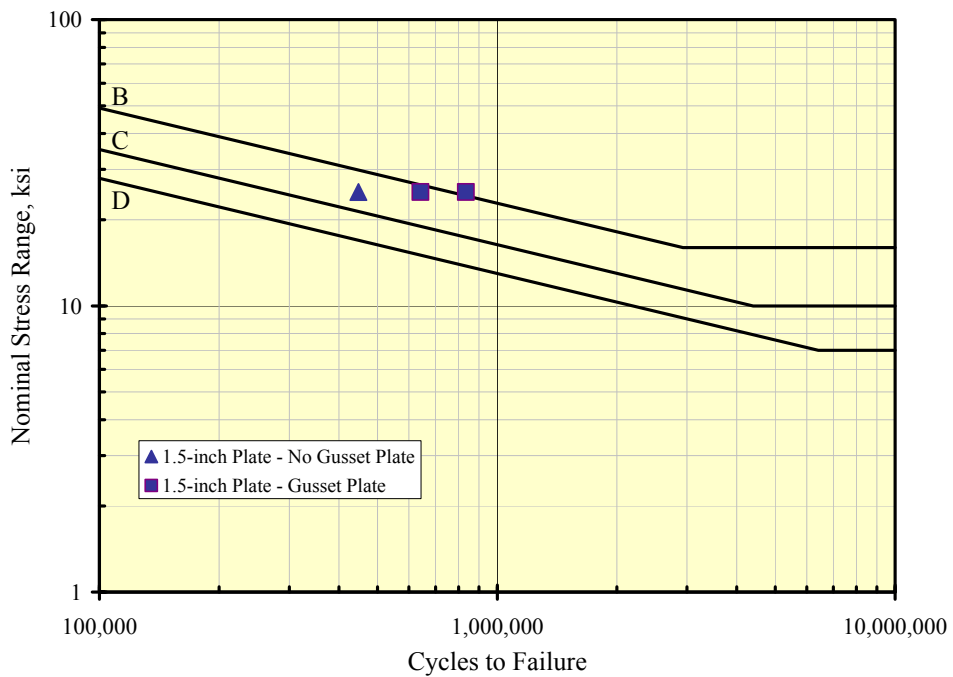


Figure 5-14. Stress Range vs. Number of Cycles to Failure for 1.5-Inch Thick Specimens.

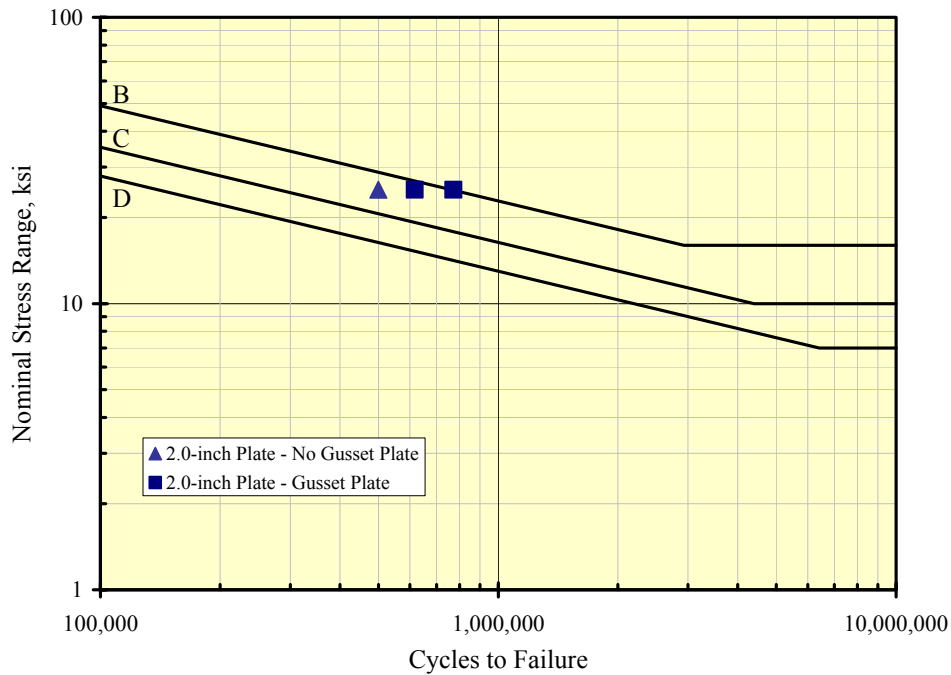


Figure 5-15. Stress Range vs. Number of Cycles to Failure for 2.0-Inch Thick Specimens.

On average, there was no significant difference in fatigue life for the drilled hole specimens without gusset plates (Figures 5-13 through 5-15). All specimens resulted in fatigue lives that ranged between Categories B and C. The specimens with bolted gusset plates resulted in an increase in the fatigue life but not enough to achieve a fatigue strength defined by Category B. This reduction in fatigue life illustrates the influence plate thickness has on the fatigue behavior of non-loaded bolted connection details.

5.6 SUMMARY

In reviewing the experimental data for the non-loaded bolted connections, the following observations and conclusions can be summarized:

- The fatigue strength of bolt holes increased with installation of pre-tensioned high-strength bolts.
- The fatigue strength of open punched holes was greater than open drilled holes for a given plate thickness.

- The fatigue strength of punched holes increased with increasing plate thickness (up to 1-inch thick plate).
- The fatigue strength of bolt holes with pre-tensioned high-strength bolts decreased with increasing plate thickness.
- No bolt hole specimen, either punched or drilled, exhibited a fatigue strength less than that defined by AASHTO Category C.

5.7 RECOMMENDATIONS

The fatigue strength of non-load-carrying bolted connections located on primary members and components should be defined by AASHTO Category C when the plate thickness of the primary member or component is 1.5 inches or greater.

CHAPTER 6: CONCLUSIONS AND RECOMMENDATIONS

The results reported herein indicate that the bending process used in the fabrication of highway girders can result in significant decreases in ductility and fracture toughness of the steel. Better control of the bending operation is needed to prevent cracking.

The test results show that application of heat during the bending process (heat-assisted cold bending) is detrimental to the ductility of the steel. Strain levels above 10 percent were difficult to achieve without necking in the specimen with the application of heat. The lowest levels of ductility were associated with test temperatures of 1100°-1200°F. Higher levels of ductility existed for specimens that simulated bending without the assistance of heat. Recommended limits of plate bending (minimum radius versus plate thickness) are given in [Table 6-1](#). Further, the use of heat during the bending process should be prohibited.

Table 6-1. Recommended Minimum Bend Radii by Plate Thickness.

Plate Thickness (inches)	Minimum Bend Radius (inches)
0.5	2.5
1	5
1.5	7.5
2	10
2.5	12.5
3	15

It must be emphasized that although there is a reduction in the ductility and fracture toughness of the steel as a result of the bending operation, the location where these bends occur in the finished bridge girder is usually non-critical. The dapped girder detail, which often requires a bent flange plate, occurs at the end of the girder where bending stresses are reduced. Therefore, the effects of bending on the behavior and performance of the flange plate are minimized. Consequently, the occurrence of cracking becomes a more important issue during fabrication than during the service life of the bridge.

Additionally, the fatigue strength of non-load-carrying bolted connections located on primary members and components should be defined by AASHTO Category C when the plate thickness of the primary member or component exceeds 1.5 inches.

To further expand the conclusions gathered through the current study, additional areas of the plate bending fabrication process should be considered. These areas include:

- Determining if the rate at which the plate is loaded during the fabrication process increases the plate's risk of developing cracking. Some research conducted by others has suggested that loading speed might play a role in the plate's susceptibility to cracking.
- Full-scale verification of the plate bending results, with the assistance of bridge fabricators, would be beneficial.

REFERENCES

- AASHTO/NSBA. (2002). "Steel Bridge Fabrication Guide Specification." *AASHTO/NSBA Steel Bridge Collaboration S 2.1-2002*, <<http://www.steelbridge.org/standards.htm>> (Nov. 18, 2004).
- ASME. (2004). *Boiler & Pressure Vessel Code*. American Society of Mechanical Engineers, New York.
- Avent, R. R. (1989). "Heat-straightening prototype damaged bridge girders." *J. Struct. Engrg.*, ASCE, 115(7), 1631-1649.
- Avent, R. R. (1992). "Designing heat-straightening repairs." *1992 National Steel Construction Conference Proceedings*, American Institute for Steel Construction, Las Vegas, NV, 2.1-2.23.
- Bala, S. R., and Malik, L. (1983). "Roll forming to higher strain levels successful." *Welding and Metal Fabrication*, 51(2), 100-108.
- Blondeau, R., Boullisset, R., Ramon, J. L., Kaplan, D., and Roesch, L. (1984). "Cold forming and welding behaviors of heavy plate steels for pressure vessel applications." *5th International Conference on Pressure Vessel Technology, Volume 2: Materials and Manufacturing*, ASME, San Francisco, CA, 1257-1289.
- Boresi, A. P., and Schmidt, R. J. (2003). *Advanced Mechanics of Materials*, Master's thesis, Texas A&M University. College Station, TX.
- Christian, L. C. (2005). *Thru-Thickness Bending Stress Distribution at Elevated Temperatures*, 6th Ed., John Wiley and Sons, New York.
- Cooke, G. M. E. (1988). "An introduction to the mechanical properties of structural steel at elevated temperatures." *Fire Safety J.*, 13, 45-54.
- FHWA. (1998). *Heat Straightening Repairs of Damaged Steel Bridges*. Federal Highway Administration, Washington D.C.
- Fry, G. T, Bailey, B. W., Farr, J. L., Elliott, J. E., and Keating, P.B. (2005). "Behavior and Design of Dapped Steel Plate Girders." Report No. 05/0-2102-1, Texas Transportation Institute, Texas A&M University System, College Station, TX.
- Kervick, R. J., and Springborn, R. K. (1966). *Cold Bending and Forming Tube and Other Sections*, American Society of Tool and Manufacturing Engineers, Dearborn, MI.
- Lie, T. T. (1992). *Structural Fire Protection*, ASCE Manuals and Reports on Engineering Practice No. 78, 224-225.

Poh, K. W. (2001). "Stress-strain-temperature relationship for structural steel." *J. Mater. Civil Engrg.*, ASCE, 13(5), 371-379.

TXDOT (2004). "2004 English Specifications Book Item 784." Texas Department of Transportation, www.dot.state.tx.us/business/specifications.htm, (Nov. 18, 2004).

TXDOT (2006) "Miscellaneous Details for Steel Girders and Beams." Texas Department of Transportation, <ftp://ftp.dot.state.tx.us/pub/txdot-info/cmd/cserve/standard/bridge/spgdste1.pdf>, (April 2006).

Weng, C. C., and White, R. N. (1990a). "Residual stresses in cold-bent thick steel plates." *J. Struct. Engrg.*, ASCE, 116(1), 24-39.

Weng, C. C., and White, R. N. (1990b). "Cold-bending of thick high-strength steel plates." *J. Struct. Engrg.*, ASCE, 116(1), 40-53.